Fus2 Localizes Near the Site of Cell Fusion and Is Required for both Cell Fusion and Nuclear Alignment during Zygote Formation

Elaine A. Elion,*‡ Joshua Trueheart,* and Gerald R. Fink*

*Whitehead Institute for Biomedical Research, Cambridge, Massachusetts 02142; and ‡Department of Biological Chemistry and Molecular Pharmacology, Harvard Medical School, Boston, Massachusetts 02115

Abstract. Zygote formation occurs through tightly coordinated cell and nuclear fusion events. Genetic evidence suggests that the *FUS2* gene product promotes cell fusion during zygote formation in *Saccharomyces cerevisiae*, functioning with the Fus1 plasma membrane protein at or before cell wall and plasma membrane fusion. Here we report the sequence of the *FUS2* gene, localization of Fus2 protein, and show that *fus1* and *fus2* mutants have distinct defects in cell fusion. *FUS2* encodes a unique open reading frame of 617 residues that only is expressed in haploid cells in response to mating pheromone. Consistent with a role in cell fusion, Fus2 protein localizes with discrete structures that could be of cytoskeletal or vesicular origin that accumulate at the tip of pheromone-induced shmoos and at the junction of paired cells in zygotes. Fus2 is predicted to be a coiled-coil protein and fractionates with a 100,000 *g* pellet, suggesting that it is associated with cytoskeleton, membranes, or other macromolecular structures. Fus2 may interact with structures involved in the alignment of the nuclei during cell fusion, because *fus2* mutants have strong defects in karyogamy and fail to orient microtubules between parental nuclei in zygotes. In contrast, *fus1* mutants show no karyogamy defects. These, and other results suggest that Fus2 defines a novel cell fusion function and subcellular structure that is also required for the alignment of parental nuclei before nuclear fusion.

MEMBRANE fusion events govern many essential processes (for review see White, 1992); intracellular fusion events mediate secretion, endocytosis, and membrane recycling in all eukaryotic cells, whereas intercellular fusion events mediate viral invasion, myotube formation, fertilization, and mating in lower eukaryotes. ER to Golgi protein routing (Pryer et al., 1992; Rothman and Orci, 1992), exocytosis (Creutz, 1992), and viral invasion (White, 1992) each involve special fusion proteins that localize at the sites of fusion and promote fusion reactions between partner lipid bilayers (White, 1992; Rothman and Warren, 1994). In many cases these proteins are conserved (Baringa, 1993). With the exception of viral invasion, little is known about the molecules that catalyze intercellular fusion events, although candidate proteins that may directly participate in sperm–egg fusion (Blobel et al., 1992; White, 1992) and cell fusion during mating (Snell, 1990; Berlin et al., 1991) have been identified.

Mating in *Saccharomyces cerevisiae* involves the fusion of two haploid cells of opposite cell type (a and α) into a diploid zygote (a/α), providing a simple model for cell and nuclear fusion (Conde and Fink, 1976; Trueheart et al., 1987). The steps leading to zygote formation have been delineated cytologically (Byers and Goetsch, 1975) and by mutations that block zygote formation (for reviews see Cross, 1988; Sprague and Thorner, 1993). Mating is initiated by cell type–specific peptide pheromones that bind receptors on cells of opposite cell type to activate a common G protein–coupled signal transduction cascade. Cells initially stimulated by low levels of pheromone activate transcription of numerous genes involved in signal transduction and fusion, resulting in cell cycle synchronization in G1 phase and reversible attachment between cells of opposite type.

Cell attachment involves the combined effects of cell surface agglutinins (Lipke and Kurjan, 1992), cell polarization toward the highest gradient of pheromone secreted by a neighboring cell of opposite mating type (Jackson and Hartwell, 1990*a*,*b*; Segall, 1993), and a partner selection system involving the receptor (Jackson et al., 1991). Cell polarization is manifested as localized cell surface growth into a projection (or shmoo), accumulation of actin cables along the growth axis (Hasek et al., 1987; Baba et al., 1989), orientation of the cytoskeleton of partner cells to-

Address all correspondence to Elaine A. Elion, Department of Biological Chemistry and Molecular Pharmacology, Harvard Medical School, 240 Longwood Avenue, Boston, MA 02115. Tel.: (617) 432-3815. Fax: (617) 738-0516.

Joshua Trueheart's current address is Cadus Pharmaceutical Corporation, 777 Old Saw Mill River Road, Tarrytown, NY 10591.

ward each other (Byers and Goetsch, 1975; Byers, 1981), new plasma membrane and cell wall at the shmoo tip (Lipke et al., 1976; Tkacz and MacKay, 1979; Field and Schekman, 1980), and enrichment of mating-specific proteins in the plasma membrane at the shmoo tip (i.e., Fus1, Trueheart et al., 1987; Ste2, Marsh and Herskowitz, 1988; Jackson et al., 1991; Ste6, Kuchler et al., 1993).

Contact between partner cells at the shmoo tips is followed by irreversible attachment and rapid fusion by coordinated cell and nuclear membrane fusion events. Cell fusion occurs between paired cell walls and plasma membranes to yield a transient heterokaryon (Conde and Fink, 1976), a step likely to involve cell wall degradation/ reorganization and localized plasma membrane fusion (Trueheart et al., 1987). Nuclear fusion occurs rapidly after cell fusion between the nuclear envelopes of parental nuclei, once the spindle pole body and associated microtubules of each nucleus have oriented toward the shmoo tip, and each nucleus has migrated to the site of cell fusion. Nuclear migration occurs through the action of cytoplasmic microtubules that extend from the spindle pole bodies of the two nuclei (Byers and Goetsch, 1975; Rose, 1991).

Without stimulation by pheromone, both cell and nuclear fusion occur at very low frequency (Curran and Carter, 1986; Rose et al., 1986). Mutations that block cell and nuclear fusion have been identified (Conde and Fink, 1976; Trueheart et al., 1987; Berlin et al., 1991; Kurihara et al., 1994), supporting the existence of proteins that catalyze these events. Mutations that block nuclear fusion but not cell fusion define genes involved in the functioning of the spindle pole body and associated microtubules (Rose, 1991) as well as fusion between nuclear envelopes (Kurihara et al., 1994). Proteins with direct functions in nuclear fusion have recently been defined in vitro (Kurihara et al., 1994; Latterich and Schekman, 1994).

Mutations in cell fusion block zygote formation at a step after cell contact and generate morphologically aberrant zygotes that retain a septum at the intersection of the joined cells (Bresch et al., 1968; Trueheart et al., 1987). Electron micrographs of the partition in aberrant zygotes shows the presence of cell wall interrupting regions of close plasma membrane apposition as might be expected for a cell fusion block (Trueheart et al., 1987). Six genes (*FUS1–3*, and *FUS5–7*) are required for cell fusion on the basis of this mutant morphology (McCaffrey et al., 1987; Trueheart et al., 1987; Elion et al., 1990; Kurihara et al., 1994). Of these, only *FUS1* and *FUS3* have been characterized to date. *FUS1* encodes an O-linked glycoprotein that spans the plasma membrane of the shmoo tip during mating, suggesting that Fus1 directly participates in cell fusion (Trueheart and Fink, 1989). *FUS3* encodes a MAP kinase with multiple functions required for signal transduction and mating (Elion et al., 1990, 1993), whose role in cell fusion is unknown.

Here, we show that Fus2 encodes a unique 617-residue protein that is expressed at a time and positioned at a site that is consistent with a role in cell fusion. Fus2 associates with novel structures that accumulate within the neck of the shmoo and near the plasma membrane at sites of cell fusion in pheromone-induced cells and in zygotes. The presence of Fus2 in zygotes is transient, and can be detected only before nuclear fusion, supporting an execution point at the time of cell fusion. Consistent with this immunolocalization pattern, Fus2 is associated tightly with cytoskeleton, membranes, or other large complexes. Although previous work suggests that Fus2 is functionally redundant with Fus1 (Trueheart et al., 1987), a comparative analysis of *fus1* and *fus2* mutants shows they have distinct defects in mating. *fus1* mutants are sensitive to low temperature and EGTA, whereas *fus2* mutants are karyogamy defective and poorly align the two parental nuclei in zygotes, as judged by a defect in microtubule alignment. Fus2 may, therefore, define a cell fusion function that is also required for proper migration of nuclei before nuclear fusion.

Materials and Methods

Microbiological Techniques

Yeast strains are listed in Table I. Gene replacement (Rothstein, 1983) and eviction/transplacement (Winston et al., 1983) were used to construct fus derivatives as described (Trueheart et al., 1987; Trueheart, 1988). Yeast media were prepared as described (Sherman et al., 1986) containing 2% dextrose, glycerol, or ethanol as indicated. Yeast extract peptone and synthetic complete media were titrated to pH 4 with HCl where indicated. Yeast transformations were performed by the method of Ito et al., 1983. Standard methods were used for bacterial transformations, plasmid DNA preparation, and plasmid constructions (Maniatis et al., 1982) using *Escherichia coli* strains HB101, C600 (Bolivar et al., 1977), and JM109 (Messing, 1982).

Plasmids Constructed

pYEE52 (*FUS2-lacZ URA3 2μ*) has the BglII–SalI fragment of Fus2 from pSB265 (Trueheart et al., 1987) subcloned into the BamHI–SalI sites of Yep357R (Myers et al., 1986). pYEE61 (*FUS2-lacZ URA3 CEN4 ARS1*) has the SalI-NcoI fragment of pYEE52 encompassing Fus2-lacZ and a portion of the *URA3* gene subcloned into the BamHI-NcoI sites of pYEE57, a derivative of YCp50 with the BamHI site converted to an SalI site by linker tailing (Lathe et al 1984). pYEE63 (*TRPE-FUS2*) has the 1.2 kb HindIII–HindIII fragment of *FUS2* subcloned into the HindIII site of pATH3 (Koerner et al., 1990).

RNA Analysis

Total RNA was isolated from *S. cerevisiae* as described (Elion and Warner, 1984). Northern analysis was performed as described (Elion et al., 1990). *FUS2* mRNA was detected with a 1.1-kb HindIII–HindIII fragment from pSB265 and *FUS1* and *ORF1* mRNAs were detected with a 6.0-kb HindIII–HindIII fragment from pSB202 (Trueheart et al., 1987). *FUS3* was detected with a 3.3-kb EcoRV–SalI fragment from pYEE94 (Elion et al., 1990). *ACT1* was detected with a 2.0-kb XhoI–HindIII fragment from pYEE15 (Elion et al., 1990). Double-stranded DNA probes were radiolabeled using random hexamers (Pharmacia Inc., Piscataway, NJ) and DNA polymerase I Klenow fragment (New England Biolabs, Beverly, MA). The direction of transcription for *FUS2* was determined by RNA dot blot analysis (Maniatis et al., 1982), using single-stranded DNA probes prepared by subcloning fragments of the *FUS2* gene into M13, mp8, and mp19 (Fig. 1), isolating single (+) strand progeny (Viera and Messing, 1987), and radiolabeling as described (Elion and Warner, 1984).

DNA Sequencing

The entire sequence of both strands of the ScaI–SalI *FUS2* fragment was determined by the dideoxy method of Sanger (1977) using single-stranded M13 phage (Messing, 1982). Sequencing reactions were electrophoresed on gradient acrylamide gels as described (Biggin et al., 1983). All predicted six base restriction sites were confirmed by restriction digestions.

Quantitative and Qualitative Mating Assays

Yeast strains were mated quantitatively and qualitatively as described (Elion et al., 1990). The frequency of diploid formation is estimated as the

number of diploids formed per total cells mated. Each frequency is the average of two matings in which at least 100 diploids were recovered. Unless noted otherwise, all matings were performed at 30°C. The effect of EGTA and Ca^{++} on mating efficiency was monitored by spotting and drying varying amounts of EGTA and Ca^{++} on YEPD plates before their use for the 4-h qualitative patch matings. Diploids were then selected on selective medium that did not contain exogenously added EGTA or Ca^{++}. The effect of temperature on mating was measured by preincubating plates used for mating at the appropriate temperature and maintaining that temperature during the mating, then selecting for diploids at 30°C. The effect of polyethylene glycol (PEG)[1] 3350 (Sigma Chemical Co., St. Louis, MO) on mating was determined in both liquid and solid medium, however, high concentrations of polyethylene glycol form an insoluble precipitate in solid agar medium, precluding interpretation of the results.

β-Galactosidase Assays

Where indicated, yeast cells were induced with 5 μM α factor for 90 min in media of pH 4 as described (Elion et al., 1990), before being assayed for β-galactosidase activity by the method of Craven et al., 1965. Cell extracts were prepared as described (Choi et al., 1994) and U of activity (nmol of *o*-nitrophenyl-galactoside cleaved/min per mg protein) were calculated by the formula: $OD_{420} \times (377.8)/\text{time (min)} \times \text{vol extract (ml)} \times \text{protein (mg/ml)}$.

Antibody Preparation

Recombinant trpE-Fus2 protein (pYEE63) was expressed in *E. coli* strain RR1 according to the method of Koerner et al., 1990. 0.2 ml of a fresh preculture grown in M9 media containing vitamin B1, ampicillin, and tryptophan was diluted into 100 ml of the same media and shaken for 2 h at 37°C, then induced with 20 μg/ml indoleacrylic acid for 4.5 h at 37°C. The culture was stored overnight on ice, pelleted, washed once in ice-cold 20 mM Tris-Cl, pH 7.4, and resuspended in 20 ml of 20 mM Tris-Cl, pH 7.4, 5 mM EDTA, 3 mg/ml lysozyme, and incubated for 2 h on ice. 1.4 ml 5 M NaCl and 1.5 ml 10% NP-40 were then added, the sample was incubated 30 min more on ice, then centrifuged for 10 min at 10,000 rpm. The pellet was dispersed with a glass rod into 20 ml ice-cold 1 M NaCl, 10 mM Tris-Cl, pH 7.4, washed once with 10 mM Tris-Cl, pH 7.4, and then suspended in 0.4 ml 2× Laemmli buffer. Samples were sonicated and boiled before electrophoresis on preparative SDS–polyacrylamide gels (10% polyacrylamide, 30%:0.8% acrylamide/bisacrylamide; 3 mm thick). Gel slices containing trpE-FUS2 were excised after brief staining with 1% Coomassie blue, finely ground, and the protein was eluted from the gel by incubation at 24°C in electrophoresis buffer. The eluate was collected and concentrated with a microcentricon 30, and protein concentration was estimated by SDS-PAGE using protein standards. Two rabbits (114 and 115, housed at the Whitehead Institute Animal Facility) were each injected three times with 0.1 mg of protein (in 0.25 ml PBS that was suspended in 0.5 ml complete Freund's adjuvent) following a standard injection and bleeding schedule. A portion of the antisera from one rabbit (115) was preadsorbed first to purfied trpE protein affixed to nitrocellulose, then affinity purified to the original trpE-Fus2 fusion protein affixed to nitrocellulose exactly as described Smith and Fisher (1984).

Preparation of Yeast Extracts

Yeast strains containing plasmids were grown at 30°C in selective synthetic complete media with 2% dextrose to an A_{600} of 0.4–0.8 and then induced for 90 min at 30°C with α factor (5 μM α factor for *SST1* strains, and 0.05 μM α factor for *sst1Δ* strains) in media that were at pH 4 as described (Elion et al., 1990). Cells were disrupted by glass beads and proteins were precipitated with TCA as described (Osashi et al., 1982). Proteins were separated on 7.5% SDS–polyacrylamide gels (Laemmli, 1970). The distribution of Fus2 in whole-cell extracts was examined essentially as described (Franzusoff et al., 1991) with several modifications. Approximately 400 ml of logarithmically growing cells in SC media (*EY957 MATa sst1Δ* at OD_{600} of 0.25) were induced with α factor for 90 min, the cells were pelleted, washed once with water, then quick frozen in ethanol/dry ice. Cells were thawed on ice and resuspended in 2 ml buffer A (20 mM MES/Tris, pH 6.5, 100 mM NaCl, 5 mM $MgCl_2$, 0.7 M sorbitol, 10 mM DTT, 0.1 μg/ml PMSF, 5 μg/ml each of pepstatin A, chymostatin, leupeptin, antipain). 0.5 ml zymolyase^{10,000} (10 mg/ml) was added, and the samples were incubated for 30 min at 30°C. Samples were kept on ice and ~0.5 vol of glass beads were added and the sample was vortexed six times for 30-s bursts until microscopic examination showed 100% disruption of cells. 0.25 ml of the disrupted cell mixture was aliquoted into five microultracentrifuge tubes (Beckman Instruments, Inc., Fullerton, CA) and 0.25 ml of each of the following buffers was added: buffer A, buffer B (A+ 1 M NaCl), buffer C (A + 2% Triton X-100), buffer D (A + 4 M urea), buffer E (A + 0.2 M $NaCO_3$, pH 11.5). The samples were vortexed briefly, incubated for 30 min on ice, vortexed again, then centrifuged at 100,000 *g* for 30 min at 4°C. The supernatants were carefully collected with a needle attached to a syringe and mixed with an equal volume of 2× sample buffer. The pellets were rinsed once with ice-cold buffer A, then suspended in 1× sample buffer to the same final volume as the supernatants, sonicating to aid suspension. 40 μl of each sample was boiled for three minutes before being resolved on an 8% SDS–polyacrylamide gel and transferred to nitrocellulose and probed with Fus2 antisera. A second, identically prepared, immunoblot was probed with an mAb to Tcm1 (ribosomal protein L3, gift of J. Warner, Albert Einstein College of Medicine).

Western Blotting

Samples were electrophoresed by SDS-PAGE on 7.5% polyacrylamide gels (acrylamide/bisacrylamide, 30:0.8), then transferred to 0.45 μm nitrocellulose (Schleicher & Schuell Inc., Keene, NH) essentially as described (Burnette, 1981). Nitrocellulose filters were blocked in TBST-milk (10 mM Tris-HCl, pH 7.4, 150 mM NaCl, 0.05% Tween-20 (Sigma Chemical Co.) 5% nonfat milk and 10 mM NaN_3) for 1–3 h at room temperature, then incubated with primary antibody for 2 h at room temperature or overnight at 4°C. Immunoblots were washed five times with TBST at room temperature, then incubated for 1–2 h with a secondary antibody diluted 1:2,000 (rabbit anti–mouse IgG (Jackson ImmunoResearch Laboratories Inc., West Grove, PA) for radioactive blots, HRP-conjugated goat anti–mouse IgG and HRP-conjugated goat anti–rabbit IgG (Bio-Rad Laboratories, Hercules, CA) for nonradioactive blots) in TBST–milk at room temperature. Immunoblots were washed five times with TBST at room temperature and then incubated with either protein A-I^{125} (Amersham Corp., Arlington Heights, IL) for 1 h and washed five times more with TBST, or developed with a chemiluminescent detection kit (Amersham Corp.) according to manufacturer's directions. Affinity-purified Fus2 antisera was used at a dilution of 1:2,000, nonaffinity-purified Fus2 antisera was used at a dilution of 1:200. mAb to β-galactosidase (gift of J. Teem) was used at a dilution of 1:500. mAb to ribosomal protein Tcm1 was used at a dilution of 1:1,000.

Immunofluorescence Microscopy

Indirect immunofluorescence was performed according to Pringle et al. (1991) with several modifications. Cultures grown in SC selective media to the middle of exponential growth phase were either treated with α factor for 90 min in YEPD or mated to cells of opposite mating type for 2–4 h at 30°C on solid YEPD media as described (Elion et al., 1990). Cells were collected, chilled on ice for 10 min, and then fixed by the addition of 40% formaldehyde to a final concentration of 4% using either freshly purchased bottled formaldehyde (Fisher Scientific Co., Pittsburgh, PA) or freshly dissolved paraformaldehyde. Cells were fixed on ice for a period ranging from 30 min to 2 h, then washed twice with solution B (100 mM potassium phosphate, pH 7.5, 1.2 M sorbitol), and resuspended at a concentration of ~1×10^8 cells/ml in solution B containing 30 μM β-mercaptoethanol, 0.1 μg/ml PMSF, 5 μg/ml each of pepstatin A, chymostatin, leupeptin, antipain. Lyticase (Enzo Biochemicals, Inc., New York) was added to 0.1 mg/ml and cells were digested for ~15 min at 30°C. The oxalolyticase was then diluted by adding three vol of ice-cold solution B, the spheroplasts were pelleted by centrifugation at 1,500 rpm at 4°C, washed twice with fresh solution B, and resuspended at 10^8 cells/ml. 10 μl of spheroplasts was pipetted onto wells of microscope slides (PolyScience Corp., Niles, IL) that had been acid washed, dried, and coated with polylysine (1 mg/ml). Spheroplasts were allowed to settle for 10 min, then the slides were incubated at −20°C in 100% methanol for 6 min, 100% acetone for 30 s. Samples were rehydrated with solution B, then incubated in solution B + protease inhibitors + 2% BSA for 1 h at 30°C. The primary antibody was added in the same buffer (affinity-purified Fus2 antisera diluted 1:5, β-galactosidase monoclonal diluted 1:50) and incubated for 2 h at room temperature; then the wells were washed five times with solution B. The samples were incubated in several dilutions of secondary antibody (1:50–1:250 dilutions of fluoroscein-conjugated affinity-purified goat anti–

1. *Abbreviation used in this paper*: PEG, polyethylene glycol.

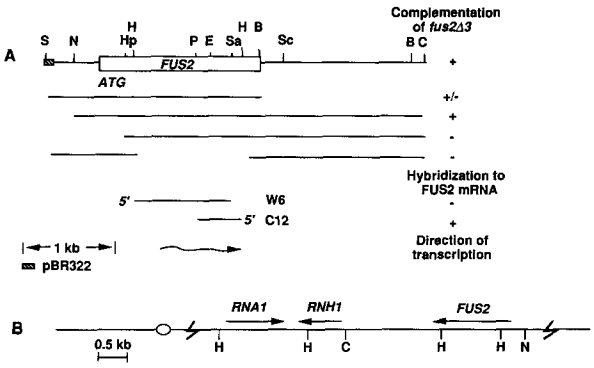

C

```
       10                  30                  50
GATCTTTTGAATTTTGCATTAAACAGTGAAGAAGGTAGTAGAGACCGTTTCAAAGTCATA

       70                  90                 110
ACAGAGTTTTTAGGTAGAGGTGCCATCAGTTATTCTGACATCACTATTTAATGATGGATC

      130                 150                 170
ATAACGATCTATTGTGCCCGCCGCGTCACAAATGCGCCCCGAACTTGTCGCGAAGTTAAT

      190                 210                 230
CTGAAACATATATGTTACCTACTGAAACAGCGCATGTTGGAAAAGACAAAGGTGAAGACG
      ======              ======

      250                 270                 290
AAGTTGTATATTTAAGATAGACCCTTTATACATCCTTTTGAAAAAATTATTAATGTGGCA

      310                 330                 350
ACCGTCTTTTATTTGACAAAGTATCTTTTTTCTTTGTGAAACCAATTTTAGGTTTTCTTG
                  ----------

      370                 390                 410
TTATAGTAAGTTCTTAAGAAAAAGACAAGAAAACCCCTTGCGATGTTTAAGACTTCATAT
                                            M  F  K  T  S  Y    6

      430                 450                 470
AACTTGTACGATTTGAACTATCCGAAAAATGATTCATTAACGCCAATAAGAGACTACAAA
N  L  Y  D  L  N  Y  P  K  N  D  S  L  T  P  I  R  D  Y  K    26

      490                 510                 530
AATGACTATTTTCATAAAAATGATGACAAATTACCAGAAATTGTTAGAAAACCTACGAGA
N  D  Y  F  H  K  N  D  D  K  L  P  E  I  V  R  K  P  T  R    46

      550                 570                 590
AAGTTATCGAAACATGAAAACAAACTCAACGATAAAAAATTCACGAATAAACGACCAGCA
K  L  S  K  H  E  N  K  L  N  D  K  K  F  T  N  K  R  P  A    66

      610                 630                 650
AGTCTGGACTTGCATTCTATAGTGGAGAGCCTGAGCAATAAAAAAATTTACTCTCCTATT
S  L  D  L  H  S  I  V  E  S  L  S  N  K  K  I  Y  S  P  I    86

      670                 690                 710
AACACAGAGATATTTCAAAATGTCGTGAGACTGAATTTGAGCCCTCAGATTCCCAATTCT
N  T  E  I  F  Q  N  V  V  R  L  N  L  S  P  Q  I  P  N  S   106

      730                 750                 770
CCTCACGAGGGATGCAAATTTTATAAAAATCGTACAGGAGTTTTACCTCTCTGAAGTGGAA
P  H  E  G  C  K  F  Y  K  I  V  Q  E  F  Y  L  S  E  V  E   126

      790                 810                 830
TATTACAATAATTTGTTAACCGCAAATAACGTATACAGAAAGGCATTGAATAGTGATCCA
Y  Y  N  N  L  L  T  A  N  N  V  Y  R  K  A  L  N  S  D  P   146

      850                 870                 890
AGATTCAAGAATAAACTTGTCAAGCTTGATTCAAGTGACGAGCTATTGCTTTTTGGGAAC
R  F  K  N  K  L  V  K  L  D  S  S  D  E  L  L  L  F  G  N   166

     1810                1830                1850
AATGCATGGAAAAAGGTGATCGAGTGCGAACGCCCTTCTGGTGCATTTTTTGCGCACGAT
N  A  W  K  K  V  I  E  C  E  R  P  S  G  A  F  F  A  H  D   486

     1870                1890                1910
AACTTAATATCGACCATGTGTTCTTCGTACATAGATAAACTGCATGAACAAAAAAATCAA
N  L  I  S  T  M  C  S  S  Y  I  D  K  L  H  E  Q  K  N  Q   506

     1930                1950                1970
GTAACAATTTTGAAACTCACAGAGCTCGAAACAGATGTGATGAACCCACTTGAAAGAATC
V  T  I  L  K  L  T  E  L  E  T  D  V  M  N  P  L  E  R  I   526

     1990                2010                2030
ATAGCCCATTGTACTACCGTTAAAAGCAAACTAAAAGATTTGCAAGCTTACATGTTATTT
I  A  H  C  T  T  V  K  S  K  L  K  D  L  Q  A  Y  M  L  F   546

     2050                2070                2090
TTACAAGAAAAAAAAAGCAAATGTGCGAGATATTAAACGTGACTTGTTGGGAATGCATTTC
L  Q  E  K  K  A  N  V  R  D  I  K  R  D  L  L  G  M  H  F   566

     2110                2130                2150
CAAAACCTGCAAAACCAGATGAAAAGGGAATTACCGGTCTTTATTACTTTGATCCCACGA
Q  N  L  Q  N  Q  M  K  R  E  L  P  V  F  I  T  L  I  P  R   586

     2170                2190                2210
TACTATCGAATGTATCTTGTTGAACTATATCAAAGTCTTCTTAAAATATTTGGAAATCAT
Y  Y  R  M  Y  L  V  E  L  Y  Q  S  L  L  K  I  F  G  N  H   606

     2230                2250                2270
TGCTGGTGGAAAAAAATACCTGCAAAAAGATCTTGAAAATATGTCTCTTAATGACTCTAT
C  W  W  K  K  I  P  A  K  R  S                              617

     2290                2310                2330
AGCTACCGGCCAAATTAAAAATCTTGATATTTTGCAGTGTTATTCTAAATCACGATATAT

     2350                2370                2390
ATGACAAAACGCATGGTAAGAAAAGATTGGCCTTTCCCTGGAGACCCTAGTGGAAGCCGT

     2410                2430                2450
GTTGTCAGAAAACTTTTCGAACTTTAACAAAAGAGTATATTTAGCTTATAGTTTTTAGAA

     2470                2490
TGTTTTGTTTTGTTTTTACTAAAGTAGTACT
```

rabbit IgG, rhodamine-conjugated affinity-purified goat anti-rabbit IgG, fluoroscein-conjugated affinity-purified rabbit anti-mouse IgG, all from Jackson ImmunoResearch Laboratories, Inc.) in solution B + protease inhibitors + 2% BSA for 2 h at room temperature in the dark. Samples were washed twice with solution B containing 0.3 M NaCl, three times with solution B. Coverslips were mounted with 90% glycerol containing 1 mg/ml *p*-phenylene diamine at pH 8.0, and 1 μg/ml 4′-6-diamidino-2-phenylindole dihydrochloride. Photomicroscopy was performed with an Axioscope (Carl Zeiss, Inc., Thornwood, NY) and Tri-X 400, Techpan 2415, and T-MAX 400 film (Eastman Kodak Co., Rochester, NY).

Results

Fus2 mRNA Is Expressed Only in the Presence of Mating Pheromone

The *FUS2* gene had been localized to a 2.5-kb ScaI–SalI fragment by complementation of the mating defect of a *MATa fus2Δ* strain (Fig. 1; Trueheart et al., 1987). Northern analysis with a probe from this region shows that the *FUS2* gene is not expressed in vegetatively growing haploid or diploid cells, but is expressed when *MATa* and *MATa/MATa* cells are treated with α factor (Fig. 2 *A*). The pattern of *FUS2* transcription resembles that of *FUS1* (McCaffrey et al., 1987; Trueheart et al., 1987), and contrasts with that of *FUS3*, which is expressed in vegetatively growing haploid cells (Elion et al., 1990). *FUS2* appears to be more tightly regulated in vegetatively growing cells than is *FUS1*, because neither longer exposure of the autoradiogram, nor hybridization of more RNA reveal any *FUS2* transcript, although low levels of *FUS1* mRNA can be detected. Induction of *FUS2* mRNA by α factor is dependent on an intact signal transduction pathway and on the Ste12 transcription factor because *FUS2* is not expressed in *fus3Δ kss1Δ*, *ste5Δ*, or *ste12Δ* strains, but is expressed in *fus3Δ* and *kss1Δ* single mutants (Fig. 2 *B*).

FUS2 Encodes a Unique Open Reading Frame

Detection of *FUS2* mRNA with single-stranded DNA probes shows that the *FUS2* gene is transcribed in the direction indicated in Fig. 1 *A*. Sequence analysis of the complementing region of DNA reveals a single open reading frame of 617 amino acids that encodes a protein of

Figure 1. Map of the *FUS2* locus and sequence of the *FUS2* gene. (*A*) *FUS2* locus as defined by restriction analysis and deletion mapping. Shown at the top is a restriction map of subclone pSB265 that complements a *fus2Δ3* strain for mating. The *FUS2* gene was localized by creating a set of deletions in pSB265. Deletions shown from top to bottom are BglII–BglII, SalI–NruI, SalI–HpaI, and HindIII–HindIII. The *fus2Δ3* allele contains a HindIII-HindIII deletion. The direction of transcription of the *FUS2* gene was determined by RNA dot blot analysis using the indicated single stranded probes, W6 and C12 (Materials and Methods). *S*, SalI; *Sa*, SacI; *N*, NruI; *H*, HindIII; *Hp*, HpaI; *P*, PvuII; *E*, EcoRI; *B*, BglII; *Sc*, ScaI; *C*, ClaI. (*B*) Chromosomal location of *FUS2*. *FUS2* maps to the right arm of chromosome 13 (Trueheart et al., 1987) next to *RNH1* and *RNA1*. Shown is a restriction map of this region (kindly provided by A. Hopper, Hershey Medical School) with the relative position of *FUS2* indicated. (*C*) Nucleotide and amino acid sequence of the *FUS2* gene. The double broken line (= = =) indicates the position of conserved TGAAACA sequences, the single broken line (- - -) indicates the homology between *FUS2* and *FUS1* in their putative promoter regions.

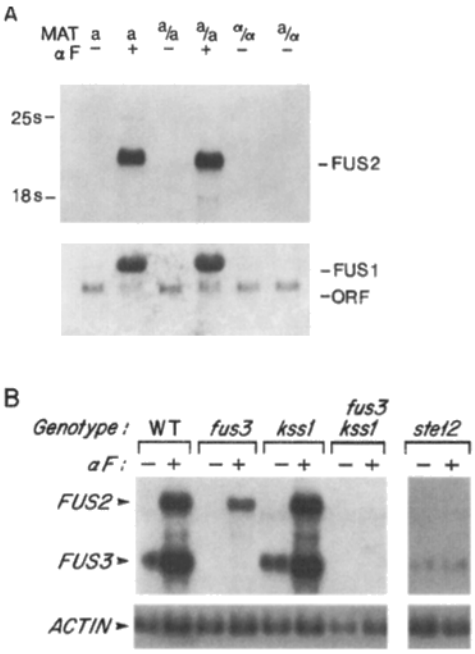

Figure 2. Northern analysis of *FUS2* transcription. (*A*) *FUS2* transcription as a function of α factor induction in *MATa*, *MATa/MATa*, *MATα/MATα*, and *MATa/MATα* cells. Total RNA was isolated and analyzed by Northern blot analysis as described (Elion and Warner, 1985). 5 μg of total RNA was loaded in each lane. A single nitrocellulose blot was hybridized first with a *FUS2* probe, then stripped and reprobed with a *FUS1/ORF* probe (Materials and Methods). − and + indicate whether strains were induced for 90 min with α factor (α F) as described in Materials and Methods. 25S and 18S indicate the positions of the corresponding rRNA in the top blot. Yeast strains are L3262 (*MATa*), L2501 (*MATa/MATa*), L2499 (*MATα/MATα*), and L2500 (*MATa/MATα*). (*B*) *FUS2* transcription in *fus3 kss1* and *ste12* strains. Northern analysis was performed exactly as described in *A*, with − and + indicating whether strains were induced for 90 min with α factor (α F) before RNA isolation. The nitrocellulose blot was first hybridized with *FUS2* and *FUS3* probes, then stripped and reprobed with an *ACT1* probe. Yeast strains are: EY699 (WT), EY700 (*fus3Δ*), EY725 (*kss1Δ*), EY723 (*fus3Δ kss1Δ*), EY718 (*ste12Δ*).

73,000 D. The open reading frame is on the same coding strand as that predicted by RNA analysis, and is of a size that agrees with the length of the *FUS2* transcript (Fig. 1 *B*). Two TGAAACA pheromone-response elements predicted to be bound by the STE12 protein (Dolan et al., 1989; Errede and Ammerer, 1989) are found upstream of the *FUS2* open reading frame. The presence of the TGAAACA repeats is consistent with the pattern of *FUS2* expression, which is dependent on Ste12 and pheromone (Fig. 2). The similar transcriptional regulation of *FUS1* and *FUS2* suggests that the two genes may share common promoter elements. Comparision of the 5′ regions of *FUS1* and *FUS2* reveals a 14-nucleotide stretch of identity (TATCTTTTTTCTTT) between the two genes located at equivalent distances from the presumptive initiation codons.

Homology searches of standard public databases and of a private database (M. Goebl, personal communication) show that the Fus2 protein is unique. No homology is found between Fus1 and Fus2 in pairwise comparisons. Fus2 lacks an obvious signal sequence based on the parameters described by Kaiser et al. (1987) and does not have an obvious transmembrane domain according to the calculations of Eisenberg et al. (1984). Secondary structure predictions suggest that Fus2 is rich in amphipathic α-helical structure and contains regions likely to form coiled coils according to the algorithm of Lupas et al. (1991). Fus2 also shows weak homology (~23% identity, 45% similarity) to several cytoskeletal proteins including the yeast myosin-like protein, Mlp1 (Kolling et al., 1993), mouse dystrophin (Bies et al., 1992), and a human kinesin-related protein (Yen et al., 1992). These homologies may be significant because they extend across the entire protein and are consistent with the secondary structure predictions.

fus1 and fus2 Mutants Have Different Sensitivities to Polymyxin B, EGTA, and Low Temperature

The absence of homology between Fus1 and Fus2 suggests the two proteins perform different cell fusion functions. We therefore determined whether *fus1* and *fus2* mutants have any distinguishing phenotypes by assessing the effects of agents known to affect membranes either in vivo or in vitro (i.e., PEG, polymyxin B, temperature, Ca^{+2}) on the ability of *fus1* and *fus2* mutants to form diploids. PEG is a potent fusogen of phospholipid vesicles (Wilschut and Hoekstra, 1984), intact mammalian cells (Pontecorvo, 1976), and yeast spheroplasts (van Solingen and van der Plaat, 1977). Polymyxin B alters membrane permeability of bacteria and yeast (Boguslawski, 1985) and interferes with agglutination during mating in yeast (Boguslawski, 1986). Temperature and Ca^{+2} affect phospholipid vesicle fusion in vitro, and Ca^{+2} is an important regulator of fusion in many systems (Stegmann et al., 1989; White, 1992).

We quantitated the ability of *MATa fus*$^-$ and *MATα fus*$^-$ strains to form diploids under conditions in which the added reagent had minimal effects on the mating of Fus$^+$ strains and little or no effect on cell viability. PEG stimulates prototroph formation two- to fourfold in matings between both Fus$^+$ and Fus$^-$ parents (Table II), suggesting PEG affects *FUS1*- and *FUS2*-independent processes. This effect is detected when cells are mated in liquid culture, suggesting that PEG brings the mating yeast cells closer together by exclusion of water as it does with liposomes (Stegmann et al., 1989). In contrast, polymyxin B inhibits prototroph formation in both *fus2* and *fus1* matings (Table III). However, a distinct difference can be observed between *fus1* and *fus2* in the Fus$^-$ × Fus$^+$ crosses: when only one parent is Fus$^-$, *fus2* strains are more sensitive than *fus1* strains.

Matings between *fus1* strains are much more cold sensitive than either wild-type or *fus2* matings (38-fold inhibition for *fus1* vs. twofold for *fus2*; Table IV). The effect of low temperature is most apparent when both parents lack *FUS1*. Likewise, the removal of Ca^{+2} and any other divalent cation by the addition of EGTA inhibits prototroph formation in crosses between *fus1* mutants, but has no effect on either wild-type or *fus2* matings (Fig. 3 *A*; note that the effect is detected best in a qualitative patch mating assay). Furthermore, the inclusion of Ca^{+2} with the EGTA

Table I. Yeast Strains Used in This Study

Strain	Genotype	Source
L2499	*MATα/MATα his4–Δ5/his4–Δ9 arg11/arg11 cry1/cry1*	G. Fink
L2500	*MATa/MATα his4–Δ5/his4–Δ9 arg11/arg11 cry1/cry1*	G. Fink
L2501	*MATa/MATa his4–Δ5/his4–Δ9 arg11/arg11 cry1/cry1*	G. Fink
L3259	*MATa ura3–52 leu2-3,112 his4–34*	G. Fink
EY699	*MATa ura3–1 trp1–1 leu2–3,112 ade2–1 his3–11,15 can1–100*	E. Elion
EY700	*fus3–6::LEU2* derivative of EY699	E. Elion
EY707	*ste12::URA3* derivative of EY699	E. Elion
EY723	*fus3–6::LEU2 kss1::URA3* derivative of EY699	E. Elion
EY725	*kss1::URA3* derivative of EY699	E. Elion
EY957	*sst1Δ* derivative of EY699	E. Elion
Isogenic derivatives of JY390		
JY390	*MATa kss1– ura3–52 trp1Δ1 his4–34*	J. Trueheart
JY387	*MATa kss1– fus2Δ3 ura3–52 trp1Δ1 his4–34*	J. Trueheart
JY417	*MATa kss1– fus1Δ1 ura3–52 trp1Δ1*	J. Trueheart
JY419	*MATa kss1– fus1Δ1 fus2Δ3 ura3–52 trp1Δ1*	J. Trueheart
JY428	*MATα kss1– fus2Δ3 ura3–52 trp1Δ1 his4–34 can^R*	J. Trueheart
JY429	*MATα kss1– fus1Δ1 fus2Δ3 ura3–52 trp1Δ1 can^R*	J. Trueheart
JY430	*MATα kss1– fus1Δ1 ura3–52 trp1Δ1 can^R*	J. Trueheart
JY431	*MATα kss1– ura3–52 trp1Δ1 his4–34*	J. Trueheart
Isogenic derivatives of JY396		
JY396	*MATα kss1– ura3–52 leu2–3,112 his4–34 [K$^+$]*	J. Trueheart
JY395	*MATα kss1– fus2Δ3 ura3–52 leu2–3,112 his4–34 [K$^+$]*	J. Trueheart
JY412	*MATα kss1– fus1Δ1 fus2Δ3 ura3–52 leu2–3,112 [K$^+$]*	J. Trueheart
JY416	*MATα kss1– fus1Δ1 ura3–52 leu2–3,112 [K$^+$]*	J. Trueheart
JY424	*MATa kss1– fus2Δ3 ura3–52 leu2–3,112 his4–34*	J. Trueheart
JY425	*MATa kss1– ura3–52 leu2–3,112 his4–34*	J. Trueheart
JY426	*MATa kss1– fus1Δ1 fus2Δ3 ura3–52 leu2–3,112*	J. Trueheart
JY427	*MATa kss1– fus1Δ1 ura3–52 leu2–3,112*	J. Trueheart
kar1–1 derivatives of Fus strains		
EY73	JY396 *kar1–1*	E. Elion
EY77	JY416 *kar1–1*	E. Elion
EY89	JY395 *kar1–1*	E. Elion
EY94	JY425 *kar1–1*	E. Elion
EY98	JY427 *kar1–1*	E. Elion
EY102	JY424 *kar1–1*	E. Elion
ρ°Cyh2^R derivatives of Fus strains		
EY81	JY396 *ρ°Cyh2^R*	E. Elion
EY82	JY395 *ρ°Cyh2^R*	E. Elion
EY83	JY412 *ρ°Cyh2^R*	E. Elion
EY84	JY416 *ρ°Cyh2^R*	E. Elion
EY85	JY424 *ρ°Cyh2^R*	E. Elion
EY86	JY425 *ρ°Cyh2^R*	E. Elion
EY87	JY426 *ρ°Cyh2^R*	E. Elion
EY88	JY427 *ρ°Cyh2^R*	E. Elion
EY260	JY424 *ρ°Cyh2^R*	E. Elion
EY262	JY425 *ρ°Cyh2^R*	E. Elion
EY264	JY426 *ρ°Cyh2^R*	E. Elion
EY266	JY427 *ρ°Cyh2^R*	E. Elion
EY268	JY395 *ρ°Cyh2^R*	E. Elion
EY270	JY412 *ρ°Cyh2^R*	E. Elion
EY272	JY416 *ρ°Cyh2^R*	E. Elion
HO switched derivatives of JY132/JY133		
JY132	*MATa ura3–52 lys2–801 trp1Δ1 his4–34*	Trueheart et al., 1987
JY133	*MATα ura3–52 leu2–3,112 his4–34*	Trueheart et al., 1987
EY310	*MATa/MATa* diploid	E. Elion
EY312	*MATα/MATα* diploid	E. Elion
EY324	EY310 + pYEE52	E. Elion
EY325	EY310 + pYEE61	E. Elion
EY326	EY310 + pSB234	E. Elion
EY327	EY310 + B929	E. Elion
EY338	EY312 + pYEE52	E. Elion
EY339	EY310 + pYEE61	E. Elion
EY340	EY310 + pSB234	E. Elion
EY341	EY310 + B929	E. Elion
Isogenic derivatives of JK103		
JK103	*MATα ura3–52 ade2–1 trp1–289 leu2–3,112 can^R cyh^R cry^R*	J. Kim
EY185	*fus1Δ1 derivative of JK103*	E. Elion
EY195	*fus2Δ3 derivative of JK103*	E. Elion
Congenic *lys9* strains		
JBY342	*MATa lys9*	J. Brill
JBY343	*MATa fus1Δ1 lys9*	J. Brill
JBY345	*MATa fus2Δ::URA3 ura3–52 lys9*	J. Brill
JBY347	*MATa fus1Δ1 fus2Δ::URA3 ura3–52 lys9*	J. Brill
JBY350	*MATα lys9*	J. Brill

restores mating in *fus1* crosses, suggesting that *fus1* mutants are more sensitive to calcium levels for optimal cell fusion. Thus, *fus1* strains are more temperature and Ca^{+2} dependent for efficient cell fusion than are wild-type and *fus2Δ* strains. These phenotypic differences suggest that *FUS1* and *FUS2* encode qualitatively different functions required for cell fusion.

fus2 Mutants Display Karyogamy Defects

The morphology of *fus1*- and *fus2*-blocked zygotes suggests they could be defective in karyogamy as well as cell fusion (Trueheart et al., 1987). Zygotes defective in nuclear fusion give rise to stable haploid cytoductants containing the cytoplasm of one parent and the nucleus of the other, thus providing a convenient way to monitor nuclear fusion genetically (Conde and Fink, 1976). We quantitated the ability of *fus* mutants to transmit cytoplasmic particles while mating, by measuring the degree of transmittance of mitochondria from one parent to another in isogenic crosses. In each case, a *MATa rho° cyh^{R}2* parent was mated to a *MATα rho$^+$ CYH2* parent, and haploid exconjugants containing the *Cyh^R* nucleus and *rho$^+$* cytoplasm were selected. *fus2* mutants exhibit a 150-fold higher frequency of cytoduction (percentage cytoductant/percentage diploid) compared with wild-type strains, whereas *fus1* × *fus1* crosses exhibit wild-type levels of cytoduction (Table V). The *fus2* crosses exhibit a significant elevation in the transmission of mitochondria to haploid exconjugants, approximately one-tenth that found for the *kar1-1* mutant (Kim et al., 1991). The frequency of cytoduction increases even further in *fus2* matings in which cell fusion is more tightly blocked (and the percentage diploids formed is decreased), to 260-fold greater for *fus1* × *fus1 fus2* matings in which only one parent *fus2* and 2,700-fold greater for *fus2* × *fus1 fus2* matings in which both parents are *fus2*.

Table II. Effect of PEG During Mating of Fus Mutants

	Percent prototrophs*		
Fus cross	YPD	6.7% PEG ^{3350}	Fold stimulation
+ × +	8.6	15.5	1.9
$1^- \times 1^-$	14.7	44.0	3.0
$2^- \times 2^-$	12.6	56.7	4.5

*Cells were grown in YPD to an A_{600} of 0.5–0.8, then diluted to an A_{600} of 0.25 with either YPD, or YPD containing 6.7% polyethylene glycol (~mol wt of 3,350). Approximately 0.5 ml of each parent was mated in a 3-ml glass tube on a roller wheel for 6 h at 30°C. Samples were then diluted into ice-cold water, sonicated, and plated in duplicate onto YPD and minimal plates to determine the total number of cells and the number of prototrophs. The concentration of PEG used did not effect cell viability.

These surprisingly high cytoduction frequencies strongly suggest that *fus2* mutants are defective at some step in nuclear fusion.

A second phenomenon associated with a block in nuclear fusion is chromo- or plasmi-duction, the transmittance of chromosomes or plasmid DNA from one parental nucleus to the other in the absence of nuclear fusion (Dutcher, 1981). For this experiment, a *MATa ura3-52* parent harboring a *URA3 CEN4* plasmid (YCp50) is mated to a *MATα ura3-52 can1^R cyh2^R* parent and *MATα* exconjugants containing YCp50 are selected. The frequency of Ura$^+$ reversion of the *ura3-52* locus in the *MATα* parent and mutation of both *CAN1* and *CYH2* to resistant alleles in the *MATa* parent is extremely low, ruling out these events as major sources of the colonies we observe. As shown in Fig. 3 *C*, plasmiduction is greatly enhanced in a *fus2* × *fus2* cross compared with *FUS2* × *FUS2* and *fus1* × *fus1* crosses. This increase in plasmiduction is similar to that seen in an isogenic *kar1-1* × *KAR1* cross (Fig. 3 *C*), in which diploids form at ~10% wild-type levels. The effects of *fus2* and *kar1* on plasmiduction are not additive, as shown by the equivalent level of plasmiduction in a *fus2* × *fus2 kar1* cross. These results substantiate the cytoduction results and suggest further that *fus2* mutants may perturb the same pathway required for nuclear fusion that is affected by a *kar1* mutation.

Parental Nuclei Misalign in fus2 Zygotes

We examined the morphology of microtubules in defective *fus2* zygotes, because nuclear fusion can be blocked by defects in the spindle pole body and associated microtubules (Rose, 1991), in addition to defects in the fusion of nuclear envelopes (Kurihara et al., 1994). Zygotes that had not yet undergone nuclear fusion were compared in Fus$^+$ × Fus$^+$ and Fus$^-$ × Fus$^-$ crosses by fixing populations of cells after they were mated for a brief time interval and then staining for microtubules and DNA. Random fields of cells containing occasional zygotes were photographed, and the zygotes were scored for position of parental nuclei and orientation of the spindle pole body and associated microtubules relative to the junction between the joined cells. In Fus$^+$ × Fus$^+$ zygotes, the parental nuclei migrate to the position of cell fusion and align with the spindle pole body and associated microtubules of each nucleus oriented toward the other (Rose and Fink, 1986). Misaligned nuclei are those in which the spindle pole bodies and associated microtubules fail to juxtapose. As shown in Table VI and Fig. 4, 100% of wild-type zygotes and 91% of *fus1* × *fus1* zygotes display an alignment of spindle pole

Table III. Effect of Polymyxin B Sulfate (PBS) on Prototroph Formation in Fus Matings

	Fold inhibition of prototroph formation*				
	Fus genotype				
PBS ug/ml	+ × +	+ × 1^-	1^- × 1^-	+ × 2^-	2^- × 2^-
1	1.8	1.7	4.6	5.5	9.0
5	1.5	2.5	37.0	20.0	40.0
10	15.5	14.0	52.0	34.0	49.0

*Cells were mated exactly as described in Table I, in either YPD, or in YPD containing the indicated amount of polymyxin B sulfate. The concentrations of PBS used did not affect cell viability. The fold inhibition by PBS was determined by dividing the frequency of prototrophs formed in the absence of PBS by the frequency of prototrophs formed in the presence of PBS. Numbers represent the average of two experiments. The relative mating frequencies between the different mutant combinations were similar to that shown in Table I. Yeast strains used: JY387, JY390, JY417, JY419, JY396, JY395, JY412, JY416.

Table IV. Effect of Low Temperature During Mating of fus Mutants

Fus cross	Percent prototrophs* 30°C	14°C	Fold inhibition
+ × +	47	28	1.7
$1^- \times 1^-$	13	0.34	38
$2^- \times 2^-$	11	3.5	3
$1^-2^- \times 1^-$	0.6	0.02	30
$1^-2^- \times 2^-$	5.3	0.5	10.6
$1 \times 1^-$	26	9	2.9
$1 \times 2^-$	29	11	2.6
$1 \times 1^-2^-$	16	4	4

*Prototroph formation was quantitated as described after a 3-h mating on YPD plates at the indicated temperature (Elion et al., 1990). The strains used in the experiment are: JBY342, JBY343, JBY345, JBY347, EYL44, EYL45, EYL46, EYL47.

bodies and microtubules judged to be normal. By contrast, the majority (79%) of *fus2* × *fus2* zygotes have misaligned nuclei. This finding is consistent with the nuclear fusion defect of *fus2Δ* mutants and suggests that *FUS2* is required for a function that affects proper alignment of the nuclei in addition to cell fusion.

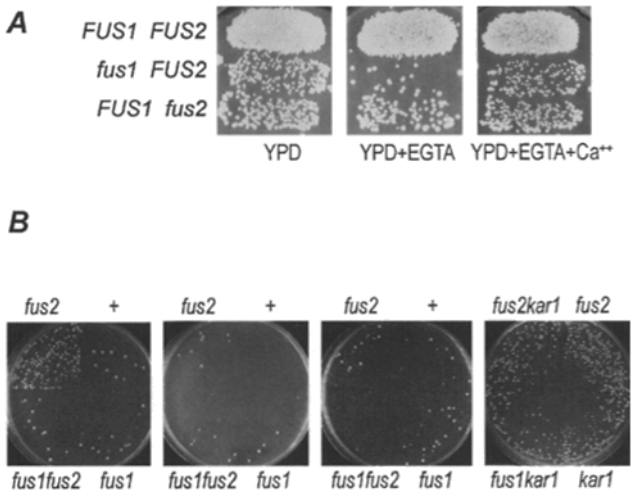

Figure 3. Qualitative patch mating tests of *fus1* and *fus2* mutants. (*A*) Effect of EGTA and Ca^{+2}. *MATa* yeast strains were grown overnight as patches on YPD plates, then mated to lawns of *MATα fus1Δ* cells for 2 h at 30°C on YPD plates with or without 7.5 mM EGTA and 7.5 mM Ca^{+2}. Diploids were then selected on YNB plates containing uracil and histidine. Note that under these conditions of brief mating, it is possible to detect significant reductions in the mating efficiency of *fus1* and *fus2* single mutant crosses, in contrast to results obtained with 4 h matings (Trueheart et al., 1987). No effects were detected in parallel matings with lawns of *MATα* and *MATα fus2Δ* strains. Yeast strains are: JY387, JY390, JY417, JY416. (*B*) Measurement of plasmiduction in *fus1*, *fus2*, and *kar1* strains. Patches of *MATa fus⁻ ura3-52 leu2-3,112 his4-34* strains harboring YCp50 were grown overnight on SC–uracil plates and mated to lawns of *MATα fus⁻ ura3-52 leu2-3,112 ade2 trp1-289 can1^R cyh2^R* strains for 4 h at 30°C. Plasmiductants were recovered by replica plating the mating cells to YNB plates containing adenine, leucine, tryptophan, canavanine, cycloheximide. Yeast strains patched are: JY424-JY427, EY94, EY98, EY102. Yeast strains used as lawns are: EY183, EY185, EY195.

Table V. Frequency of Cytoduction in fus Crosses

Parents	Percent Diploid*	Percent Cytoductant‡	Percent Cytoductant/ Diploid
a rho° Cyh^R × *α rho⁺ Cyh^S*			
+ × +	50.3	0.211	0.00419
$1^- \times 1^-$	28.4	0.172	0.00606
$2^- \times 2^-$	31.8	19.4	0.610
$1,2^- \times 1^-$	0.0103	0.0115	1.117
$1,2^- \times 2^-$	0.0160	0.182	11.38

*Prototroph and cytoductant formation were quantitated by mass matings as described (Elion et al., 1990) after a 4-h mating at 30°C.
‡Cytoductants were selected on solid YEP medium containing 3% glycerol, 0.05% glucose, and 3 μg/ml cycloheximide as described (Berlin et al., 1990). The strains used in the experiment are: EY85, EY86, EY87, EY88, JBY342, JBY343, JBY345.

Detection of Fus2 Protein in α Factor–induced Cells

To characterize Fus2 in vivo, we constructed a FUS2–β-galactosidase fusion (*FUS2–lacZ*) and raised an antiserum against an internal portion of Fus2 fused to the *E. coli* TRPE protein (Materials and Methods). The *FUS2–lacZ* fusion contains the entire *FUS2* open reading frame and partially complements the mating defect of a *fus2Δ* mutant, but does not suppress a *fus1Δ* mutant, unlike native Fus2 (Trueheart et al., 1987). Immunoblot analysis of yeast whole-cell extracts shows that the Fus2 antisera recognizes a protein of ~70 kD in cells that have been exposed to α factor, consistent with the predicted mass of Fus2 and the pattern of transcription of the *FUS2* gene (Fig. 5, *A* and *B*). That this protein is Fus2 is supported by the fact that (*a*) it is not present in *fus2Δ* cells that have been induced by α factor, (*b*) its abundance increases in cells that harbor a multicopy plasmid containing the *FUS2* gene, and (*c*) the FUS2–β-galactosidase fusion protein of the predicted size is recognized by both the Fus2 antisera

*Table VI. Tally of Microtubule Distribution in Fus⁺ and Fus⁻ Zygotes**

Genotype‡	Total zygotes scored	Number zygotes with unfused nuclei	Number aligned MTs in unfused nuclei	Percent misaligned nuclei
FUS × FUS	33	18	18	0
fus1 × fus1	25	23	21	8.7
fus2 × fus2	19	19	4	79

*Microtubule distribution in zygotes was assessed as follows: yeast strains were grown exponentially at 30°C in YEPD to an OD_{600} of 0.25–0.35. To mate, ~2.5 OD U of cells of parents were pelleted together, resuspended in 0.1 ml of supernatant, and transferred onto a 60 × 15 mm YEPD agar plate. Cells were mated briefly for 2 h at 30°C, then collected in 5 ml liquid YEPD, fixed with formaldehyde, and prepared for indirect immunofluorescence as described in Materials and Methods. Nuclear DNA was visualized by staining with the dye DAPI, microtubules were visualized with YOL1/34 mAb. Fields of cells containing zygotes were photographed at random for analysis. Microtubule alignment was defined as whether the spindle pole bodies of adjacent (paired) nuclei in zygotes were oriented towards each other in the same plane of focus. Misaligned parental microtubules were considered not to be oriented towards each other and/or in different planes of focus. The reduced number of *fus1* × *fus1* and *fus2* × *fus2* zygotes tallied may reflect the fact that these zygotes are hypersensitive to the zymolyase treatment used in preparation of the cells for indirect immunofluorescence, causing lysis at the septum between paired cells.
‡The strains used in the matings were: JY425 × JY396 (*Fus* × *Fus*); JY427 × JY416 (*fus1* × *fus1*); JY395 × JY424 (*fus2* × *fus2*).

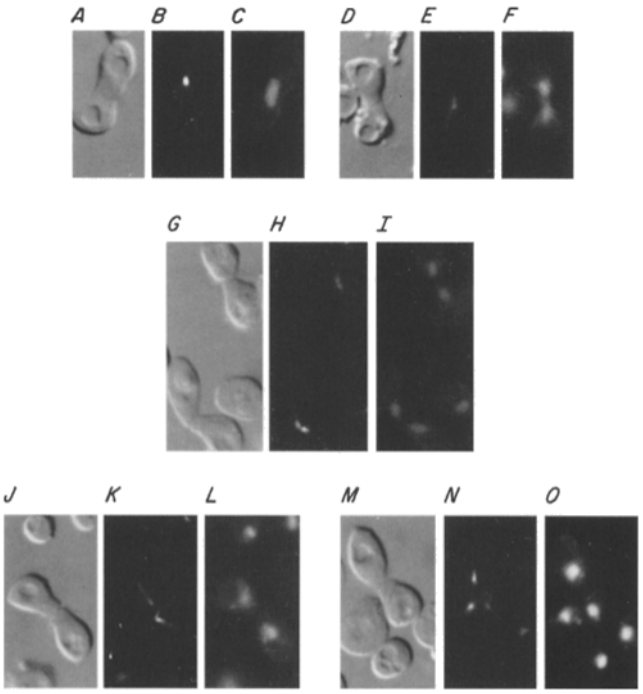

Figure 4. Morphology of nuclei and microtubules in wild-type and Fus⁻ zygotes that have not undergone nuclear fusion. *fus2Δ* × *fus2Δ* zygotes display misaligned parental nuclei as evidenced by nonaligned spindle pole bodies and associated microtubules. Shown are a representative wild-type zygote after nuclear fusion (*A–C*) and prenuclear fusion (*D–F*), two *fus1Δ* × *fus1Δ* zygotes prenuclear fusion (*G–I*), and two *fus2Δ* × *fus2Δ* zygotes prenuclear fusion (*J–L*, *M–O*). Note that for both wild-type and *fus1Δ* × *fus1Δ* zygotes the spindle pole bodies have aligned towards each other in the same plane, whereas they are not pointed towards each other in the *fus2Δ* × *fus2Δ* zygotes. Panels display zygotes by DIC (*A*, *D*, *G*, *J*, *M*), microtubules by indirect immunofluorescence against β-tubulin (*B*, *E*, *H*, *K*, *N*), and nuclei by DAPI (*C*, *F*, *I*, *L*, *O*). Yeast strains used are: JY395, JY396, JY416, JY424, JY425, JY427. Cells were mated for 2 h before being fixed.

and a β-galactosidase mAb (Fig. 5, *A* and *C*). The similarity in mass between the predicted Fus2 protein and the protein recognized by the antiserum suggests that Fus2 is not grossly modified by asparagine-linked glycosylation. Consistent with this conclusion, tunicamycin treatment of α factor–induced cells does not affect the mobility of the Fus2 protein (data not shown).

Fus2 Localizes at the Shmoo Tip in Pheromone-induced Cells

Fus2 was visualized in mating yeast cells by indirect immunofluorescence using the Fus2–lacZ fusion protein and a β-galactosidase mAb. Two additional β-galactosidase fusion proteins served as integral controls, a Fus1–LacZ fusion previously shown to localize to the plasma membrane at the projection tips of pheromone-induced cells (Trueheart et al., 1987; Trueheart and Fink, 1989) and a cytoplasmic β-galactosidase protein expressed from a *HIS4* promoter. All three proteins are present in essentially equal abundance in α factor–induced cells (Fig. 5 *C*).

Fus2–lacZ localizes in punctate spots that resemble vesicles or other large structural elements such as the cytoskeleton. The spots accumulate within the projection neck at or near the projection tip of cells that have been exposed to α factor for 90 min (*A*). A small amount of cytoplasmic staining is also seen in addition to the staining within the projection. The asymmetric pattern of Fus2–lacZ distribution is readily visible in cells that have not yet undergone projection formation (Fig. 6 *A*, *top row*) indicating that the structure with which Fus2–lacZ associates is present before projection formation. In addition, the position of Fus2–lacZ does not appear to correlate with the position of the nucleus. The highly asymmetric distribution pattern of Fus2–lacZ is not an artifact of the heightened sensitivity of the projection tips to treatment by zymolyase (and thus better access to the antibody), because identically treated cells harboring the His4-LacZ fusion exhibit diffuse cytoplasmic staining of an intensity that is proportional to cell volume (*C*). Furthermore, the punctate distribution of Fus2–lacZ contrasts sharply with that of Fus1–lacZ, which localizes in a sharp rim at the tip of projections, suggesting the two proteins do not colocalize (*B*).

The distribution of native Fus2 was also examined with the affinity-purified Fus2 antibodies, because the β-galactosidase segment of the Fus2–β-galactosidase fusion could interfere with proper localization of Fus2. Initial studies to detect native Fus2 with this antibody in haploid *MATa FUS2* strains were unsuccessful, despite the fact that the Fus2–lacZ protein could be readily visualized with the Fus2 antibody, even when the *FUS2–lacZ* gene was maintained on a centromeric plasmid. Since both *FUS2–lacZ* and *FUS2* are expressed from identical promoters, the Fus2–lacZ fusion protein may be more stable than Fus2 (Fig. 5 *A*). However, we were able to detect Fus2 in diploid *MATa/MATa FUS2/FUS2* cells after α factor induction and in populations of mating *MATa/MATa FUS2/FUS2* and *MATα/MATα FUS2/FUS2* cells (Fig. 7). Visualization was greatly enhanced when the cells contained extra copies of the *FUS2* gene (on a multicopy plasmid). Fus2 distribution in these cells (Fig. 7 *A*, *d–f*) is very similar to that of Fus2-lacZ (Fig. 7 *A*, *a–c*) with one exception. The majority of native Fus2 is found at the projection tip, close to the plasma membrane, with a smaller fraction detected in the middle of the projection in occasional cells of strains harboring the *FUS2* multicopy plasmid (*d–f*). In contrast, the Fus2-lacZ protein is more often detected in the middle of projections as well as at the tip (compare two cells in *b* and *c*). We conclude that native Fus2 associates with structures that accumulate at or near the plasma membrane of projection tips. The Fus2–lacZ protein may cause the accumulation of these structures within the neck of the projection (note the Nomarski micrograph which shows surface bumps that appear to superimpose over the Fus2–lacZ staining; Fig. 6 *A*, bottom two cells).

Fus2 Localizes at the Junction of Paired Cells in Zygotes That Have Not yet Undergone Nuclear Fusion

Fus2 localization was also examined in zygotes at various stages after cell fusion in short-term matings. Strikingly, Fus2 was detected at the junction of joined cells in zygotes that had undergone cell fusion but not nuclear fusion, with similar results for wild-type zygotes and zygotes harboring

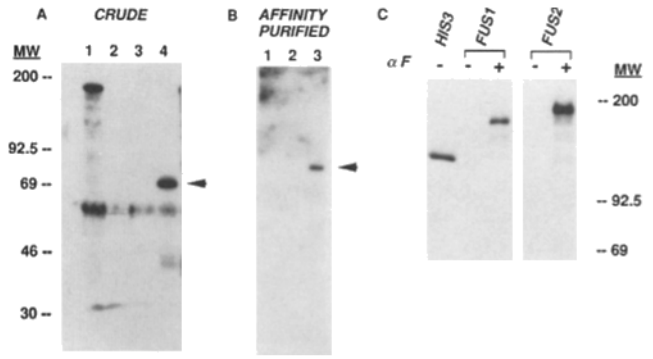

Figure 5. Immunoblot analysis of Fus2 and Fus2-lacZ. (*A*) Detection of Fus2 and Fus2-lacZ with crude antisera. 10 ml of logarithmically growing cells (A_{600} of 0.5) in SC–uracil media were induced for 2 h with α factor. Samples were collected and extracts prepared by TCA precipitation (Materials and Methods). Approximately 1/10 of extract recovered was separated on a 7.5% polyacrylamide gel (acrylamide/bis, 30:0.8). Immunoblot analysis was performed with crude anti-Fus2 antisera (at a dilution of 1:200) and ^{125}I-protein A. The arrow indicates the position of Fus2. *B* is a different immunoblot than shown in *A*, and the position of Fus2 in this immunoblot is consistent with its predicted size. The lower band is a nonspecific cross-reacting species found in all strains tested. (Lane *1*) JY425 (*FUS2*) + *FUS2-lacZ* (pYEE52) + α factor; (lane *2*) JY424 (*fus2Δ*) + Yep24 + α factor; (lane *3*) JY425 + *FUS1-lacZ* (pSB234) + α factor; (lane *4*) JY425 + *FUS2* 2μ (pSB257) + α factor. (*B*) Detection of Fus2 with affinity-purified antisera. Fus2 antisera was affinity purified (Materials and Methods) and used to detect Fus2 in an immunoblot prepared exactly as in *A*. The affinity purified antisera was used at a dilution of 1:2,000. Note that a small amount of protein of the same size as that detected in lane *3* could be visualized in lane *2* in a long exposure (data not shown). Asterisk (*) indicates position of Fus2. (lane *1*) JY424 (*fus2Δ*) + α factor; (lane *2*) JY425 (*FUS2*) + α factor; (lane *3*) JY425 (*FUS2*) + *FUS2* (pYBS257) + α factor. (*C*) Detection of His4-lacZ; Fus1-lacZ, and Fus2-lacZ with anti-β-galactosidase mAb. Yeast strain JY132 containing either B929, pSB234, pYEE52, or YCp50 was grown in SC–uracil medium and extracts prepared as described in *A*. Immunoblot analysis was performed with an anti-β-galactosidase mAb. (Lane *1*) His4-lacZ; (lane *2*) Fus1-lacZ; (lane *3*) Fus1-lacZ + α factor; (lane *4*) Fus2-lacZ; (lane *5*) Fus2-lacZ + α factor.

a *FUS2* multicopy plasmid (Fig. 7 *B*, compare *a* with *c*). Overexpression of *FUS2* increases the amount of Fus2 protein at the junction of joined cells, with little effect on the amount of cytoplasmic staining, suggesting the majority of Fus2 reaches the junction. The position of Fus2 in these zygotes suggests that it is inside the cell rather than the outer surface, consistent with the pattern observed in pheromone-induced cells. This distribution is different from that found with Fus1–LacZ that decorates the plasma membrane around the periphery of the zygote (Trueheart et al., 1987; Elion and Fink, data not shown). Furthermore, Fus2 could not be detected in zygotes that had undergone nuclear fusion, suggesting that the protein is degraded in zygotes with fused nuclei, either because it is intrinsically unstable or degraded as a consequence of nuclear fusion. The timing and localization of Fus2 are thus highly consistent with a cell fusion execution point.

Fus2 Is Enriched in a High Speed Pellet

The immunolocalization patterns of both Fus2 and Fus2-lacZ suggest that Fus2 is associated with a macromolecular structure, such as large vesicles or cytoskeleton. Indeed, preliminary attempts to assay Fus2–lacZ activity shows it is enriched in an insoluble fraction, since 90% of the β-galactosidase activity was detected in the pellet derived from a 16,000 *g* centrifugation of glass-bead disrupted cells (Table VII).

The proportion of native Fus2 associated with soluble and insoluble cell fractions was determined by separating yeast extracts by a 100,000-*g* centrifugation into pellet and supernatant and analyzing each fraction by immunoblot analysis with the Fus2 antibody. The vast majority of Fus2 is found in the pellet, indicating it is not a soluble protein (Fig. 8). The small amount of Fus2 in the supernatant may represent the fraction of the protein not associated with the structures seen by indirect immunofluorescence. As a control, the same fractions were examined for the distribution of the ribosomal protein Tcm1, also predicted to be in the pellet because of its association with ribosomes which sediment at 100,000 *g*. As predicted, all of the Tcm1 protein is in the pellet. To determine whether Fus2 is loosely associated with the insoluble fraction, extracts were treated with salt, nonionic detergent, denaturant, or high pH before centrifugation, conditions typically used to distinguish membrane-associated proteins (Fig. 8, Franzusoff et al., 1990). Fus2 was very poorly extracted from the pellet under all the conditions used, except for limited extraction with 1% Triton X-100, suggesting it is tightly associated with an insoluble fraction that could either be membraneous or cytoskeletal. Tcm1 was more readily extracted with NaCl and sodium carbonate, consistent with an association with ribosomes.

Discussion

Fus2 Localizes to a Site Consistent with a Role in Cell Fusion

Several lines of evidence, taken together, are consistent with a role for Fus2 in cell fusion. First, *FUS2* is expressed only in the presence of pheromone (Fig. 2), indicating that Fus2 carries out a function required after signal transduction. Second, Fus2 localizes at or near the site of cell fusion in mating cells. In shmoos, Fus2 associates with punctate structures that accumulate at the plasma membrane of the projection tip (Fig. 7), the site of cell fusion. In early zygotes, Fus2 localizes at the interface between joined partner cells that have undergone cell fusion but not nuclear fusion. Third, the presence of Fus2 is specific to early zygotes and is not found in late zygotes that have already undergone nuclear fusion. Thus, Fus2 is expressed at a time and positioned at a site that is consistent with a role in cell fusion that occurs before the fusion of nuclei.

Fus2 Identifies a Novel Structure at the Shmoo Tip

Fus2 associates with punctate structures that resemble vesicles in that they appear spherical (Fig. 7). Preliminary fractionation indicates Fus2 is largely insoluble, consistent with an association with either membranes or cytoskeleton (Fig. 8). The structures appear to be significantly larger than the Fus1–LacZ-associated structures that accumulate within the cytoplasm of cells treated for 2 h with α factor

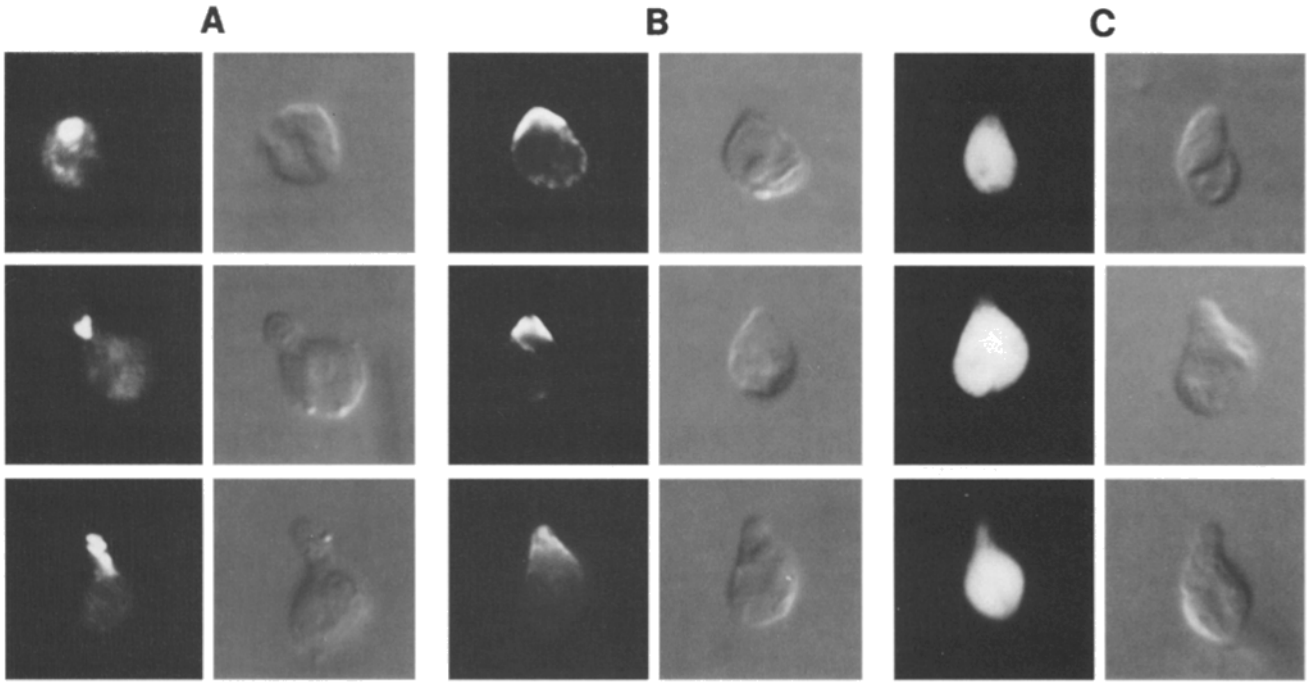

Figure 6. Distribution of Fus2-lacZ, Fus1-lacZ, and His4-lacZ in α factor–induced cells. Three representative shmoos are shown in each panel. (*A*) Fus2-lacZ. (*B*) Fus1-lacZ, (*C*) His4-lacZ. Panels show shmoos by DIC and lacZ fusion proteins by indirect immunofluorescence with an mAb to β-galactosidase. Cells were induced for 90 min with α factor before being fixed. Yeast strains are JY132 containing either pYEE61 (*FUS2-lacZ CEN*), pSB234 (*FUS1-lacZ 2μ*), or B929 (*HIS4-lacZ 2μ*).

(and are presumably secretory vesicles, Trueheart and Fink, 1989), suggesting they are distinct (Elion, E. A., and G. R. Fink, data not shown). Observation of Fus2 at different time points after α factor induction, suggests that these structures are distributed asymmetrically in projectionless cells, as well as cells that have formed a projection. Thus, they may identify a structure that either migrates to the projection tip or marks the point at which projection formation occurs. Ste6, the α factor transporter localizes in large structures resembling vesicles at the plasma membrane of the projection tip (Kuchler et al., 1993; Kolling and Hollenberg, 1994), suggesting a possible compartment for Fus2. However, these vesicles are found throughout the cell and are present constitutively. Furthermore, the relatively poor extraction of Fus2 with 1% Triton X-100 may point more to an association with a cytoskeletal element. Spa2 and Bem1, cell polarity determinants known to affect cytoskeletal structure and to be required for projection formation and mating (Gehrung and Snyder, 1990; Chenevert et al., 1992, 1994) also reside at the projection tip and could colocalize with Fus2 or be required for its localization. Interestingly, cells expressing the Fus2–lacZ fusion protein (which appears to be more stable than Fus2) often have somewhat more enlarged and elongated projections compared with wild-type cells (Figs. 6 and 7), raising the possibility that Fus2 and/or its associated structure affects projection formation. It will be of interest to determine whether Fus2 associates with a novel vesicle or cytoskeletal structure that plays a specific role in cell fusion.

Fus2 Is Required for Nuclear Alignment in Addition to Cell Fusion

We find that *fus2* mutants are clearly defective in nuclear fusion as measured by cytoduction and plasmiduction (Table V, Fig. 3), demonstrating that Fus2 has a second function required for dipoid formation that is distinct from Fus1. The nuclear fusion defect may be due to the fact that *fus2* zygotes improperly align their parental nuclei before nuclear fusion (as shown by nonaligned microtubules emanating from the spindle pole bodies of the parental nuclei; Fig. 4, Table VI), rather than a defect in fusion of the nuclear envelopes. *fus2Δ* thus defines a novel class of inefficient maters that shares features of both nuclear congression defective *kar* mutants (Kurihara et al., 1994) and cell fusion defective *fus* mutants (Trueheart et al., 1987; McCaffrey et al., 1987). Our results suggest the intriguing possibility that Fus2 operates at a step that intersects cell and nuclear fusion, events previously thought to be coordinated. Such coordination might involve attachment of the microtubules along contact points at the projection tip to ensure proper nuclear migration before or during cell fusion, and is consistent with the site of Fus2 localization. Fus2 could either be physically involved in microtubule alignment or catalyze a cell fusion step that must first take place in order for nuclear alignment to occur. We note that *spa2* mutants that are severely defective in projection formation also exhibit a modest defect in nuclear fusion as measured by cytoduction (Gehrung and Snyder, 1992), suggesting that this phenotype may be shared by mutations affecting polarization at the projection tip.

FUS1 and FUS2 Reveal Different Cell Fusion Functions

Three lines of genetic evidence previously suggested that *FUS1* and *FUS2* are functionally redundant: (*1*) overexpression of *FUS2* partially suppresses a *fus1* mutant and

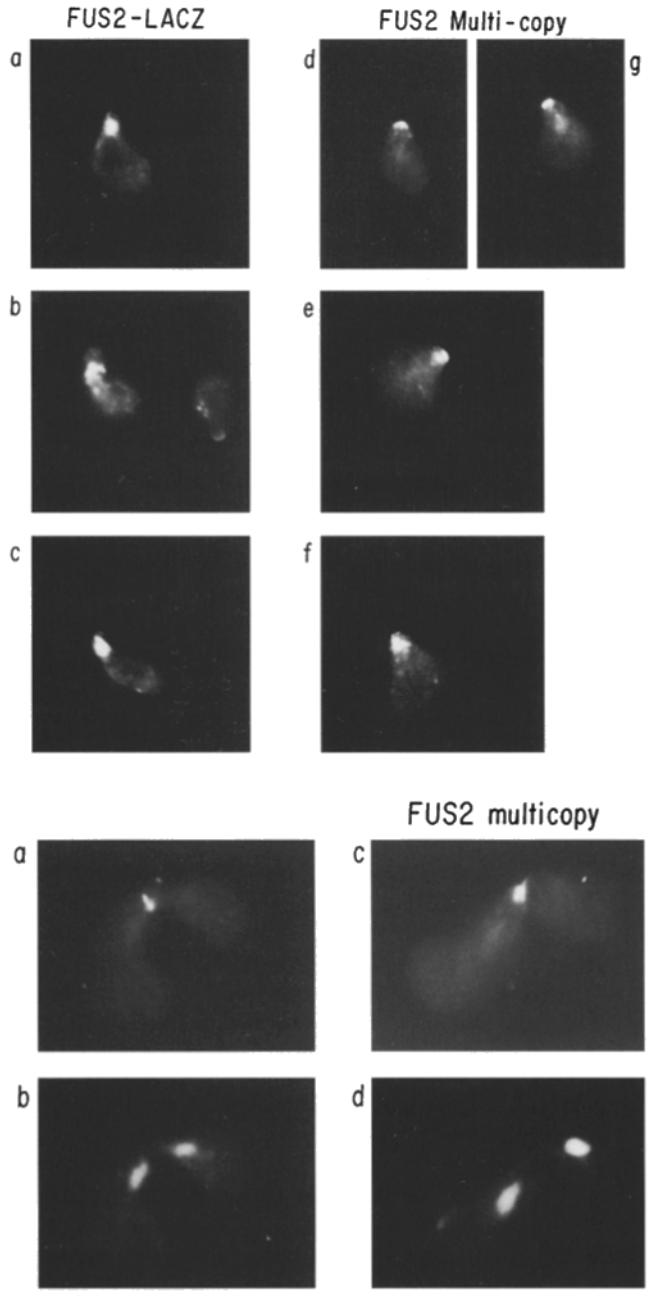

Figure 7. Distribution of Fus2 in shmoos and zygotes from a mating mixture. (*A*) Representative shmoos of cells containing either Fus2-LacZ or Fus2 on a multicopy plasmid. Panels show Fus2-LacZ and Fus2 by indirect immunofluorescence using affinity-purified antisera to Fus2 (see Materials and Methods). Cells are recovered from after a 2-h mating between *MATa/MATa* (EY310) and *MATα/MATα* (EY312) cells containing either pYEE61 (*FUS2-LacZ CEN*) or pSB257 (*FUS2* 2μ). *a–c*: Shmoos with Fus2-LacZ. *d–f*: Shmoos with excess Fus2. (*B*) Representative tetraploid zygotes. Panels show a zygote containing wild-type levels of Fus2 (*a–b*) and a zygote containing excess Fus2 (*c–d*). *a* and *c* show indirect immunofluorescence with affinity-purified Fus2 antisera, and *b* and *c* show the corresponding nuclei by DAPI. Cells are recovered from a 2-h mating between EY310 and EY312 with or without pSB257 in both parents.

Table VII. FUS2–β–galactosidase Activity by Chloroform or Glass Bead Disruption Method

LacZ fusion‡	Uninduced supernatant	Uninduced pellet	Induced supernatant	Induced pellet
	Units of activity* × 10^{-2}			
FUS2–LacZ	0.49	4.8	16.4	177.6
FUS1–LacZ	0.24	1.4	14.0	218.5
HIS4–LacZ	43.8	73.3	46.5	108.2

**MATa* cells (strain JY425) harboring *LacZ*-fusion genes grown to at an A_{600} of 0.4–0.6 were induced with 5μM α factor for 90 min before being assayed as described in Materials and Methods. Uninduced cells were treated identically by the addition of an equal volume of methanol. Units of activity are determined as described in Materials and Methods.

‡Genes encoding the *LacZ* fusion proteins were carried on *URA3* 2μ plasmids pYEE52 (*FUS2*), pSB234 (*FUS1*, Trueheart et al., 1987), B543 (*HIS4*).

vice versa, (*2*) *fus1* and *fus2* mutant zygotes are morphologically similar, and (*3*) a *fus1fus2* double mutant is >1,000-fold more defective in mating than either single mutant (Trueheart et al., 1987). We show here that *FUS1* and *FUS2* most likely perform qualitatively different cell fusion functions and define distinct components of the cell fusion pathway. First, the predicted Fus2 protein bears no sequence similarity to the Fus1 protein. Second, as summarized in Table VIII, *fus1* and *fus2* null mutants have nonidentical phenotypes. *fus2* mutants are defective in nuclear fusion and alignment of microtubules as well as more sensitive to polymyxin b, a compound that affects agglutination and membrane permeability. In contrast, *fus1* mutants undergo normal nuclear fusion and are hypersensitive to low temperature and depletion of calcium during mating. Third, Fus1 and Fus2 appear to have different sites of localization at the shmoo tip, and neither protein is required for the other's localization (Elion, E. A., and G. R. Fink, data not shown).

Three different models can be compared as explanations for the functional similarity between *FUS1* and *FUS2* with respect to cell fusion. In the first model, *FUS1* and *FUS2* carry out the same step in cell fusion, and the different phenotypes reflect different properties of the Fus1 and Fus2 proteins. For example, Fus2 may be more calcium- and cold-sensitive than Fus1, whereas Fus1 may be more sensitive to agents that affect agglutination and/or membrane permeability than Fus2. However, this model does not explain the different localization of the two proteins and the fact that *FUS1* is not required for nuclear fusion. In the second model, *FUS1* and *FUS2* function at different steps in a single cell fusion pathway. For example, *FUS1* could define an earlier step (consistent with Fus1 localization across the cell membrane and the cell surface), whereas *FUS2* defines a later step that is more dependent upon prior cell attachment and intersects with events required for nuclear fusion (consistent with the apparent localization of Fus2 inside the cell). However, if both genes are in the same pathway it is difficult to explain the finding that a *fus1 fus2* mutant is far more defective in cell fusion than either single mutant. In the third model, *FUS1* and *FUS2* function in parallel cell fusion pathways, with *FUS2* performing a second function required for nuclear fusion. This explanation best explains the phenotypes of single and double *fus* mutants, the different localization of Fus1 and Fus2, and the distinctive nuclear alignment defect of

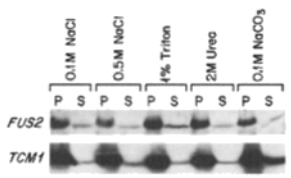

Figure 8. Association of Fus2 with a 100,000-*g* pellet. Approximately 140 ODs of logarithmically growing EY957 harboring pSB257 (*FUS2* 2μ) was induced for 90 min with 50 nM α factor, then pelleted and an extract was prepared by the glass bead/spheroplast method of Franzusoff et al. (1992) (see Materials and Methods for details). Aliquots of extract were incubated in the presence of 0.1 M NaCl, 1% Triton X-100, 2 M urea, or 0.1 M $NaCO_3$ for 1 h on ice, then centrifuged at 100,000 *g* for 30 min. Pellet and supernatant equivalents were then analyzed for the presence of Fus2 (using Fus2 antisera) and Tcm1 (using a Tcm1 mAb) on a single immunoblot.

fus2 mutants. The identification of additional proteins required for cell fusion will help distinguish between these different models.

What Is the Function of Fus2?

The phenotypes of *fus2* mutants coupled with the cytological localization of Fus2 protein argue strongly that Fus2 promotes some aspect of fusion at the projection tip and may have a direct physical role in cell fusion and karyogamy. One possibility is that Fus2 is associated with specialized vesicles that fuse with the plasma membrane to effect cell fusion and perhaps also coordinate nuclear fusion. For example, this type of vesicle might be analogous to the large exocytotic vesicles of chromaffin and neural cells or the acrosomal vesicles that fuse with sperm plasma membrane during the acrosome reaction of fertilization (Yanagimachi, 1988). Such specialized vesicles could either deliver enzymes that promote cell fusion or remove cell wall material to allow plasma membrane fusion. As yet there is no biochemical evidence for regulated secretory vesicles in yeast (Prior et al., 1992), although the subcellular distribution of Ste6 suggests the existence of a nonclassical vesicular pathway to the shmoo tip (Kolling and Hollingberg, 1994). A second possibility is that Fus2 is part of a cytoskeletal (or other) structural component that is required for both cell fusion and nuclear fusion, and is consistent with the predicted coiled coil nature of Fus2, its weak sequence homology to myosin-related proteins. Such a structure, assembled at the site of cell fusion at the shmoo tip, might organize the fusion machinery, prevent cytoplasmic leakage, and aid in the proper alignment of extranuclear microtubules required for an ensuing nuclear fusion event. Both interpretations posit that Fus2 interacts, directly or indirectly, with proteins required for nuclear fusion and projection formation. The identification of the proteins associated with Fus2 will help distinguish between alternative explanations of Fus2 function.

Table VIII. Summary of Mating Phenotypes of Fus Mutants

	FUS	*fus1*	*fus2*
Stimulation by PEG	+	++	+++
Inhibition by PBS	−	++	+++
Inhibition by low temperature	+/−	++	+/−
Inhibition by EGTA	−	+	−
Enhanced Cytoduction	−	−	++
Enhanced Plasmiduction	−	−	++
Microtubule misalignment	−	+/−	++

We thank A. Hopper for providing mapping information, J. Teem for anti-β-galactosidase antibody, J. Warner for anti-Tcm1 antibody, A. Adams for helpful advice on immunofluorescence, and J. Chenevert and J. Pringle for discussion of unpublished data concerning *BEM1*. We also thank S. Kron for comments on the manuscript.

This research was supported by a Helen Hay Whitney Fellowship to E. A. Elion, National Institutes of Health grant GM35010 to G. R. Fink, and start-up funds from Harvard Medical School to E. A. Elion.

Received for publication 17 February 1995 and in revised form 10 July 1995.

References

Baba, M., N. Baba, Y. Ohsumi, K. Kanaya, and M. Osumi. 1989. Three dimensional analysis of morphogenesis induced by mating pheromone α factor in *Saccharomyces cerevisiae*. *J. Cell Sci.* 94:207–216.

Baringa, M. 1993. Secrets of secretion revealed. *Science (Wash. DC).* 260:487–489.

Berlin, V., J. A. Brill, J. Trueheart, J. D. Boeke, and G. R. Fink. 1991. Genetic screens and selections for cell and nuclear fusion mutants. *Methods Enzymol.* 194:774–792.

Biggin, M. D., T. J. Gibson, and G. F. Hong. 1983. Buffer gradient gels and S^{35} as an aid to rapid DNA sequence determination. *Proc. Natl. Acad. Sci. USA.* 80:3963–3965.

Bies, R., S. F. Phelps, M. D. Cortez, R. Roberts, C. T. Caskey, and J. S. Chamberlain. 1992. Human and murine dystrophin mRNA transcripts are differentially expressed during skeletal muscle, heart, and brain development. *Nucleic Acids Res.* 20:1725–1731.

Blobel, C. P., T. G. Wolfsberg, C. W. Turck, D. G. Myles, P. Primakoff, and J. M. White. 1992. A potential fusion peptide and an integrin ligand domain in a protein active in sperm–egg fusion. *Nature (Lond.).* 356:248–252.

Boguslawski, G. 1985. Effects of polymyxin B sulfacte and olymyxin B nonapeptide on growth and permeability of the yeast *Saccharomyces cerevisiae*. *Mol. & Gen. Genet.* 199:401–405.

Boguslawski, G. 1986. Polymyxin B nonapeptide inhibits mating in *Saccharomyces cerevisiae*. *Antimicrob. Agents Chemother.* 29:330–332.

Bolivar, F., R. L. Rodriguez, T. J. Greene, M. C. Betlach, H. L. Heyneker, and H. W. Boyer. 1977. Construction and characterization of new cloning vehicles. II. A multipurpose cloning system. *Gene (Amst.).* 2:95–113.

Bresch, C., G. Muller, and R. Egel. 1968. Genes involved in meiosis and sporulation of a yeast. *Mol. & Gen. Genet.* 102:301–306.

Burnette, W. N. 1981. Western blotting: Electrophoretic transfer of proteins from sodium dodecyl sulfate polyacrylamide gels to unmodified nitrocellulose and radiographic detection with antibody and radio-iodinated protein A. *Anal. Biochem.* 112:195–203.

Byers, B., and L. Goetsch. 1975. The behavior of spindles and spindle plaques in the cell cycle and conjugation of *Saccharomyces cerevisiae*. *J. Bacteriol.* 124:511–523.

Byers, B. 1981. Cytology of the yeast life cycle. *In* The Molecular Biology of the Yeast Saccharomyces: Life Cycle and Inheritance. J. Strathern, E. Jones, and J. Broach, editors. Cold Spring Harbor Laboratory, Cold Spring Harbor, NY. 59–96.

Chenevert, J., K. Corrado, A, Bender, J. Pringle, and I. Herskowitz. 1992. A yeast gene (*BEM1*) necessary for cell polarization whose product contains two SH3 domains. *Nature (Lond.).* 356:77–79.

Chenevert, J., N. Valtz, and I. Herskowitz. 1994. Identification of genes required for pheromone-induced cell polarization in *Saccharomyces cerevisiae*. *Genetics.* 136:1287–1296.

Choi, K-Y., B. Satterberg, D. Lyons, and E. A. Elion. 1994. Ste5 tethers multiple protein kinases in the MAP kinase cascade required for mating in *S. cerevisiae*. *Cell.* 78:499–512.

Conde, J., and G. R. Fink. 1976. A mutant of *Saccharomyces cerevisiae* defective for nuclear fusion. *Proc. Natl. Acad. Sci. USA.* 73:3651–3655.

Craven, G. R., E. J. Steers, J. L. Bethune, and C. B. Anfinsen. 1965. Purification, composition, and molecular weight of the β-galactosidase of *Escherichia coli* K12. *J. Biol. Chem.* 240:2468–2477.

Creutz, C. 1992. The annexins and exocytosis. *Science (Wash. DC).* 258:924–930.

Cross, F., L. H. Hartwell, C. Jackson, and J. B. Konopka. 1988. Conjugation in *Saccharomyces cerevisiae*. *Annu. Rev. Cell Biol.* 4:429–457.

Curran, B. P. G., and B. L. A. Carter. 1986. α-factor enhancement of hybrid formation by protoplast fusion in *Saccharomyces cerevisiae* II. *Curr. Genet.* 10: 943–945.

Dolan, J. W., C. Kirkman, and S. Fields. 1989. The yeast STE12 protein binds to the DNA sequence mediating pheromone induction. *Proc. Natl. Acad. Sci. USA.* 86:5703–5707.

Dutcher, S. K. 1981. Internuclear transfer of genetic information in the *kar1-1/KAR1* heterozygotes of *Saccharomyces cerevisiae*. *Mol. Cell. Biol.* 1:245–253.

Eisenberg, D., E. Schwarz, M. Komaromy, and R. Wall. 1984. Analysis of mem-

brane and surface protein sequences with the hydrophobic moment plot. *J. Mol. Biol.* 179:125–142.

Elion, E. A., and J. R. Warner. 1984. The major promoter element of rRNA transcription lies 2 kb upstream. *Cell.* 39:663–673.

Elion, E. A., P. L. Grisafi, and G. R. Fink. 1990. *FUS3* encodes a cdc2/CDC28-related kinase required for the transition from mitosis into conjugation. *Cell.* 60: 649-664.

Elion, E. A., B. Satterberg, and J. A. Kranz. 1993. *FUS3* phosphorylates multiple components of the mating signal transduction cascade: evidence for STE12 and FAR1. *Mol. Biol. Cell.* 4:495–510.

Errede, B., and G. Ammerer. 1989. STE12, a protein involved in cell-type specific transcription and signal transduction in yeast is part of protein-DNA complexes. *Genes & Dev.* 3:1349–1361.

Field, C., and R. Schekman. 1980. Localized secretion of acid phosphatase reflects the pattern of cell surface growth in *Saccharomyces cerevisiae*. *J. Cell Biol.* 86:123–128.

Franzusoff, A., J. Rothblatt, and R. Schekman. 1991. Analysis of polypeptide transit through the secretory pathway. *Methods Enzymol.* 194:662–674.

Gehrung, S., and M. Snyder. 1990. The *SPA2* gene of *Saccharomyces cerevisiae* is important for pheromone-induced morphogenesis and efficient mating. *J. Cell Biol.* 111:1451–1464.

Hasek, J., I. Rupes, J. Svobodova, and E. Streiblova. 1987. Tubulin and actin topology during zygote formation of *Saccharomyces cerevisiae*. *J. Gen. Microbiol.* 133:3355–3363.

Ito, H., Y. Fukada, K. Murata, and A. Kimura. 1983. Transformation of intact yeast cells with alkali cations. *J. Bacteriol.* 153:163–168.

Jackson, C. L., and L. H. Hartwell. 1990*a*. Courtship in *S. cerevisiae*: both cell types choose mating partners by responding to the strongest pheromone signal. *Cell.* 63:1039–1051.

Jackson, C. L., and L. H. Hartwell. 1990*b*. Courtship in *Saccharomyces cerevisiae*: an early cell-cell interaction during mating. *Mol. Cell. Biol.* 10:2203–2213.

Jackson, C. L., J. B. Konopka, and L. H. Hartwell. 1991. *S. cerevisiae* pheromone receptors activate a novel signal transduction pathway for mating partner discrimination. *Cell.* 67:389–402.

Kaiser, C. A., D. Preuss, P. Grisafi, and D. Botstein. 1987. Many random sequences functionally replace the secretion signal sequence of yeast invertase. *Science (Wash. DC).* 235:312–317.

Kim, J., P. O. Ljungdahl, and G. R. Fink. 1991. Kar-enhancing mutations (kem) affect nuclear fusion during conjugation and microtubule and spindle pole body function during mitosis in *Saccharomyces cerevisiae*. *Genetics.* 126:799–812.

Koerner, T. J., J. E. Hill, A. M. Myers, and A. Tzagoloff. 1990. High-expression vectors with multiple cloning sites for construction of trpE-fusion genes. *Methods Enzymol.* 194:477–490.

Kolling, R., and C. P. Hollenberg. 1994. The ABC-transporter Ste6 accumulates in the plasma membrane in a ubiquinated form in endocytosis mutants. *EMBO (Eur. Mol. Biol. Organ.) J.* 13:3261–3271.

Kolling, R., T. Nguyen, E. Y. Chen, and D. Botstein. 1993. A new yeast gene with a myosin-like heptad repeat structure. *Mol. & Gen. Genet.* 237:359–369.

Kuchler, K., H. G. Dohlman, and J. Thorner. 1993. The a-factor transporter (*STE6* gene product) and cell polarity in the yeast *Saccharomyces cerevisiae*. *J. Cell Biol.* 120:1203–1215.

Kurihara, L. J., C. T. Beh, M. Latterich, R. Schekman, and M. D. Rose. 1994. Nuclear congression and membrane fusion: two distinct events in the yeast karyogamy pathway. *J. Cell Biol.* 126:911–924.

Laemmli, U. K. 1970. Cleavage of structural proteins during the assembly of the head of bacteriophage T4. *Nature (Lond.).* 227:680–685.

Lathe, R., M. P. Kieny, S. Skory, and J. P. Lecocq. 1984. Linker tailing: unphosphorylated linker oligonucleotide for joining DNA termini. *DNA (NY).* 3: 173–182.

Latterich, M., and R. Schekman. 1994. The karyogamy gene *KAR2* and novel proteins are required for ER–membrane fusion. *Cell.* 78:87–98.

Lipke, P. N., and J. Kurjan. 1992. Sexual agglutinins in budding yeasts: structure, function and regulation of yeast cell adhesion proteins. *Microbiol. Rev.* 56:180–194.

Lipke, P. N., A. Taylor, and C. E. Ballou. 1976. Morphogenic effects of α-factor on *Saccharomyces cerevisiae* cells. *J. Bacteriol.* 127:610–618.

Lupas, A., M. Van Dyke, and J. Stock. 1991. Predicting coiled coils from protein sequences. *Science (Wash. DC).* 252:1162–1164.

Maniatis, T., E. F. Fritsch, and J. Sambrook. 1982. Molecular Cloning: A Laboratory Manual. Cold Spring Harbor Laboratory, Cold Spring Harbor, NY. 545pp.

Marsh, L., and I. Herskowitz. 1988. From membrane to nucleus: the pathway of signal transduction in yeast and its genetic control. *Cold Spring Harbor Symp. Quant. Biol.* 53:557–565.

McCaffrey, G., F. J. Clay, K. Kelsay, and G. F. Sprague. 1987. Identification and regulation of a gene required for cell fusion during mating of the yeast *Saccharomyces cerevisiae*. *Mol. Cell. Biol.* 7:2680–2690.

Messing, J. 1982. Construction of improved m13 vectors using oligonucleotide-directed mutagenesis. *In* Genetic Engineering: Principles and Methods, Vol. 4. J. K. Setlow and A. Hollaender, editors. Plenum Publishing Corp., New York. 19-34.

Myers, A. M., A. Tzagoloff, D. M. Kinnery, and C. J. Lusty. 1982. Yeast shuttle and integrative vectors with multiple cloning sites suitable for construction of lacZ fusions. *Gene (Amst.).* 45:299–310.

Osashi, A., J. Gibson, I. Gregor, and G. Schatz. 1982. *J. Biol. Chem.* 262:13042–13047.

Pontecorvo, G. 1976. Polyethylene glycol (PEG) in the production of mammalian somatic cell hybrids. *Cytogenet. Cell Genet.* 16:399–400.

Pringle, J. R., A. E. M. Adams, D. G. Drubin, and B. K. Haarer. 1991. Immunofluorescence methods for yeast. *Methods Enzymol.* 194:565–601.

Pryer, N. K., L. J. Wuestehube, and R. Schekman. 1992. Vesicle-mediated protein sorting. *Annu. Rev. Biochem.* 61:471–516.

Rose, M. D. 1991. Nuclear fusion in yeast. *Annu. Rev. Microbiol.* 45:539–567.

Rose, M. D., B. Price, and G. R. Fink. 1986. *Saccharomyces cerevisisae* nuclear fusion requires prior activation by alpha factor. *Mol. Cell. Biol.* 6:3490–3497.

Rothman, J. E., and L. Orci. 1992. Molecular dissection of the secretory pathway. *Nature (Lond.).* 355:409–415.

Rothman, J. E., and G. Warren. 1994. Implications of the SNARE hypothesis for intracellular membrane topology and dynamics. *Curr. Biol.* 4:220–223.

Rothstein, R. 1983. One-step gene disruption in yeast. *Methods Enzymol.* 101: 202–211.

Sanger, F., S. Nicklen, and A. R. Coulson. 1977. DNA sequencing with chain termination inhibitors. *Proc. Natl. Acad. Sci. USA.* 74:5463–5467.

Segall, J. E. 1993. Polarization of yeast cells in spatial gradients of α mating factor. *Proc. Natl. Acad. Sci. USA.* 90:8332–8336.

Sherman, F., G. R. Fink, and J. B. Hicks. 1986. Methods in Yeast Genetics. Cold Spring Harbor Laboratory, Cold Spring Harbor, NY. 120 pp.

Smith, D. E., and P. A. Fisher. 1984. Identification, developmental regulation, and response to heat shock of two antigenically related forms of a major nuclear envelope protein in *Drosophila* embryos: application of an improved method for affinity purification of antibodies using polypeptides immobilized on nitrocellulose blots. *J. Cell Biol.* 99:20–28.

Snell, W. J. 1990. Adhesion and signalling during fertilization in multicellular and unicellular organisms. *Curr. Opin. Cell Biol.* 2:821–832.

Sprague, G. F., Jr., and J. W. Thorner. 1994. Pheromone response and signal transduction during the mating process of *Saccharomyces cerevisiae*. *In* The Molecular and Cellular Biology of the Yeast *Saccharomyces*. Cold Spring Harbor Laboratory, Cold Spring Harbor, NY. 657–744.

Stegmann, T., R. W. Doms, and A. Helenius. 1989. Protein-mediated membrane fusion. *Annu. Rev. Biophys. Biophys. Chem.* 18:187–211.

Tkacz, J. S., and V. L. MacKay. 1979. Sexual conjugation in yeast. *J. Cell Biol.* 80:326–333.

Trueheart, J. 1988. Molecular and genetic analysis of two genes required for yeast cell fusion. Ph.D. thesis. Massachusetts Institute of Technology, Cambridge, MA. 175 pp.

Trueheart, J., J. D. Boeke, and G. R. Fink. 1987. Two genes required for cell fusion during conjugation: evidence for a pheromone-induced surface protein. *Mol. Cell. Biol.* 7:2316–2328.

Trueheart, J., and G. R. Fink. 1989. The yeast cell fusion protein FUS1 is O-glycosylated and spans the plasma membrane. *Proc. Natl. Acad. Sci. USA.* 86: 9916–9920.

van Solingen, P., and J. B. van der Plaat. 1977. Fusion of yeast spheroplasts. *J. Bacteriol.* 130:946–947.

Viera, J., and J. Messing. 1987. Production of single-stranded DNA. *Methods Enzymol.* 153:3–11.

White, J. M. 1992. Membrane fusion. *Science (Wash. DC).* 258:917–924.

Wilschut, J., and D. Hoekstra. 1984. Membrane fusion: from liposomes to biological membranes. *TIBS (Trends Biochem. Sci.).* 9:479–483.

Winston, F., F. Chumley, and G. R. Fink. 1983. Eviction and transplacement of mutant genes in yeast. *Methods Enzymol.* 101:211–227.

Wolfsberg, T. G., F. J. Bazan, C. P. Blobel, D. G. Myles, P. Primakoff, and J. M. White. 1993. The precursor region of a protein active in sperm–egg fusion contains a metalloprotease and a disintegrin domain: structural, functional and evolutionary implications. *Proc. Natl. Acad. Sci. USA.* 90:10783–10787.

Yanagimachi, R. 1988. Sperm–egg fusion. *Curr. Top. Membr. Transp.* 32:3–43.

Yen, R., T. J. Li, B. T. Schaar, I. Szilak, and D. W. Cleveland. 1992. CENP-E is a putative kinetochore motor that accumulates just before mitosis. *Nature (Lond.).* 359:536–539.